Time-Dependent Weighting of Neutron Kinetics Equations

Application of Time-Dependent Weighting to Solution of Neutron Kinetics Equations

by

GARY KURT ALBERT, B. Eng.

A Report
Submitted to the School of Graduate Studies
in Partial Fulfillment of the Requirements for
the Degree
Master of Engineering

McMaster University
1982

MASTER OF ENGINEERING (1982) McMaster University
Hamilton, Ontario

TITLE: Application of Time-Dependent Weighting to Solution of Neutron Kinetics Equations

AUTHOR: G.K. Albert, B. Eng. (McMaster University, Hamilton)

SUPERVISOR: Dr. D.A. Meneley

NUMBER OF PAGES: vi, 88

Abstract

The calculation, storage and usage of the adjoint function as a weight function in the point kinetics calculations represents a significant portion of the final cost of large reactor transient analysis. Replacement of this function with the shape function would reduce this cost component considerably.

Arguments supporting just such a replacement in the point kinetics equations are developed using a time dependent weighting function and implemented in the Improved QuasiStatic method. A one dimensional diffusion code was written to test this scheme and the results are presented.

Acknowledgements

At this time I would like to extend my thanks to all of my friends who would not let me give up when times were bad. I would particularly like to thank my parents and compatriates of B105 of the Nuclear Research Building for their support.

I would also like to thank Dr. D.A. Meneley for his patience and guidance throughout my studies and Dr. D. Thompson for the push that resulted in this report.

Table of Contents

	Page
Abstract	iii
Acknowledgements	iv
Table of Contents	v
Table of Figures	vi
Introduction	1
The Point Kinetics Equations	4
The Weight Function	9
The Improved QuasiStatic Approximation (I.Q.S.)	15
The Self-Adjointness Assumption	18
The One Dimensional Diffusion Code	20
Solution of the Finite Difference Equations	27
The Transient Algorithm	29
Results and Discussion	39
Conclusions	44
Appendix A (Results)	45
References	88

Table of Figures

		Page
Fig. 1	Finite difference mesh point structure	21
Fig. 2	Test cast material region configuration	45
Fig. 3	Case number 1 time zero neutron flux shape	47
Fig. 4	Case number 1 adjoint flux shape	48
Fig. 5	Case 1 option 1 results	51
Fig. 6	Case 1 option 2 results	53
Fig. 7	Case 1 option 4 results	55
Fig. 8	Case number 2 time zero neutron and adjoint flux shape	57
Fig. 9	Case 2 option 1 results	59
Fig. 10	Case 2 option 2 results	61
Fig. 11	Case 2 option 3 results	63
Fig. 12	Case 2 option 4 results	65
Fig. 13	Case number 3 time zero neutron flux shape	67
Fig. 14	Case number 3 adjoint flux shape	68
Fig. 15	Case 3 option 1 results	70
Fig. 16	Case 3 option 2 results	72
Fig. 17	Case 3 option 3 results	74
Fig. 18	Case 3 option 4 results	76
Fig. 19	Case number 4 adjoint flux shape	78
Fig. 20	Case number 4 adjoint flux shape	79
Fig. 21	Case 4 option 1 results	81
Fig. 22	Case 4 option 2 results	83
Fig. 23	Case 4 option 3 results	85
Fig. 24	Case 4 option 4 results	87

Introduction

The development of numerical methods in Reactor Kinetics problems has been historically closely coupled with the development of modern computer technology. Before any appreciable computer capability was available, the complexity and size of the problems to be solved were kept necessarily small. Intuative approaches in hand and computer relaxation methods along with restrictive approximations limited the range and validity of solveable problems. Even relatively simple reactor configurations do not lend themselves to analytical solution. Numerical solutions were the only feasable approach to solving the increasingly complex reactor configuration being studied.

As the computational capabilities of the computer system increased so accordingly did the size of problems engineers and scientists wished to solve. Eventually computor capabilities allowed them to solve very large numerical problems based on very rigourous mathematical and physical foundations. Any size problem could conceivably be solved to desired accuracy at a cost. This rather large cost component of the solution process led researchers to seek solutions based on less rigourous methods giving reasonably accurate results at reduced cost relative to the larger exact methods. Intuative approaches used in precomputor days once again played an important role in the new codes being developed. Also acceleration methods such as over and under relaxation[1] commonly used in hand relaxation methods were formally incorporated into existing codes.

These intuative approaches often based themselves on observable trends. For instance it was recognized that the solution to one problem previously solved, or a set of such solutions could well be applied to the problem at hand resulting in such methods as the Modal and Variational[2] methods. Also it was observed that for

a great many transients that the shape of the neutron flux varied only slightly from the initial condition during the transient with the major component of the change being in the amplitude or power resulting in the point kinetics based models such as the Improved Quasistatic Model[3]. In the case of very large reactors, it was evident that the criticality of a given region of the reactor was not directly dependent on the criticality of its neighbours leading to the development of such methods as the Nodal[4] methods where the problem is divided into several very large nodes each of which is coupled to its neighbours by suitable coupling coefficients based on the average flux within the node. The spacial flux shape within these nodes then being calculated by some relatively cheap method.

Since many of these methods are dependent upon an apriori knowledge of the characteristics of the problem at hand, they may be restricted to a limited set of problems. Others are more universally applicable provided peculiarities of the problem to be solved have been accounted for. The success of any such scheme however, can only be determined by comparing its results with suitable benchmark cases usually solved by the more expensive but accurate exact methods. Unless improvements in cost or convenience of application over existing methods can be demonstrated the new method must be considered unsuccessful.

One such scheme, which had originally been developed to solve problems in fast reactor kinetics, is the Improved QuasiStatic (I.Q.S.)[3] method, which has also been successfully applied to thermal reactor kinetics problems. The success of this scheme in both systems is generally recognized but the question arises whether or not the direct application of the I.Q.S. method to thermal reactor kinetics is the most efficient application or if some particular characteristic of this system can be exploited to further enhance this solution scheme.

Since we are particularly concerned with the CANDU type reactor in the Canadian nuclear industry, we will turn our attention towards answering this question with particular reference to problems

typical to Candu reactors. The Point Kinetics equations being an essential component of the I.Q.S. method provides an appropriate starting point for this search.

The Point Kinetics Equations

In developing the point kinetics equations we will follow the notation and development presented in Henry[5] with the generalization of allowing time dependence of the weight function as well as the shape function in the derivation. The starting point of this derivation will be the time dependent neutron diffusion and precursor equations which have been adopted as the foundation of present day thermal reactor analysis.

From Henry these equations are:

$$\nabla \cdot D\nabla\Psi - A\Psi + \sum_j \chi^j (1-\beta^j) F^j \Psi + \sum_{i=1}^{I} \chi_i \lambda_i c_i + q = \frac{1}{v} \frac{\delta \Psi}{\delta t} \qquad 1$$

$$\sum_j \beta_i^j F^j \Psi - \lambda_i c_i = \frac{\delta c_i}{\delta t} \qquad 2$$

where the operators A and F are defined as

$$Af = \Sigma_t(r,E,t) f(r,E,t) - \int_0^\infty \Sigma_s(r,E' \to E,t) f(r,E',t) dE' \qquad 3$$

$$F^j f = \int_0^\infty \nu^j \Sigma_f^j(r,E',t) f(r,E',t) dE' \qquad 4$$

The basic premise of the point kinetics equations is the assumption that the neutron density can be represented as a product of a time dependent amplitude function and a shape function which is nearly time independent. This near space and time separability is based on the observation that for many transients the flux shape changes only slightly from its original shape and generally rises or

falls as a whole depending on the reactivity of the system after the initial perturbation. This phenomena lies in the fact that the lifetime of a neutron in a critical assembly is on the order of a few microseconds and its mean free path for interaction is relatively large. Therefore, any change in material properties within the system must occur on a relatively long time scale with respect to the neutron lifetime and the effect on the neutron distribution would be almost instantaneous allowing the shape to rise or fall for the duration of the transient provided no further material perturbations occur. This is particularly true in fast reactors where the neutron lifetime is very short and the mean free path very large. In thermal reactors where the delayed neutrons play a significant role in any transient, the shape transient is effectively delayed enhancing this assumption although the neutron lifetime can be relatively long, particularly in heavy water moderated reactors such as the Candu. As a measure of this amplitude we introduce the amplitude function defined as:

$$T(t) = \int dV \int_0^\infty dE\ W(r,E,t)\frac{1}{v}\psi(r,E,t) \qquad 5$$

where the weight function W(r,E,t) is introduced only to generalize the definition at the present time. We will note that this function is defined over the same space, energy and time interval as the neutron flux. Having defined our amplitude function, we can now define the shape function as:

$$S(r,E,t) = \psi(r,E,t)/T(t) \qquad 6$$

also defined over the same domain as the neutron flux. Substituting the neutron flux defined by equation (6) into equation (1), adding and subtracting the term

$$\sum_j \sum_{i=1}^{I} \chi_i \beta_i^j F^j \psi(r,E,t) \qquad 7$$

in equation (1), multiplying through by our time dependent weight function and integrating over all energies and space we have the result:

$$T\int W\nabla\cdot D\nabla S - T\int WAS + T\int W\sum_j\left(\chi_p^j(1-\beta^j) + \sum_{i=1}^{I}\chi_i\beta_i^j\right)FS - \qquad 8$$

$$T\int W\sum_j\sum_{i=1}^{I}\chi_i\beta_i^j FS + \int W\sum_{i=1}^{I}\chi_i\lambda_i c_i + \int Wq = \int W\frac{1}{v}\frac{\delta ST}{\delta t}$$

where functional dependencies have been left out for simplicity. Similarly by multiplying equation (2) by $W(r,E,t)\chi_i^j$ and integrating we have:

$$T\int W\sum_j\chi_i\beta_i^j F^j S - \int W\chi_i\lambda_i c_i = \int W\chi_i\frac{\delta c_i}{\delta t} \qquad 9$$

Now returning to the definition of the amplitude function and making the substitution of equation (6) we have the result:

$$T(t) = \int dV\int_0^\infty dE\ W(r,E,t)\frac{1}{v}S(r,E,t)T(t) \qquad i,\ 10$$

$$= T(t)\int dV\int_0^\infty dE\ W(r,E,t)\frac{1}{v}S(r,E,t) \qquad ii$$

therefore

$$\int dV\int_0^\infty dE\ W(r,E,t)\frac{1}{v}S(r,E,t) = 1.0 \qquad 11$$

Equation (11) expresses a necessary condition for the validity of the point kinetics result. This of course would be true if the shape and weight functions were time independent, which was one of the

assumptions made at the beginning of this development. With this in mind, and by making appropriate rearrangements in equations (8) and (10), we can define the terms:

$$\Gamma(t) = \int W\left\{\sum_j \chi_p^j((1-\beta^j) + \sum_{i=1} \chi_i \beta_i^j) F^j S\right\} \qquad 12$$

$$\rho(t) = \frac{1}{\Gamma(t)}\left\{ \int W(\nabla \cdot D\nabla S - AS) + \Gamma(t)\right\} \qquad 13$$

$$\beta_i(t) = \frac{1}{\Gamma(t)} \int W \sum_j \chi_i \beta_i^j F^j S \qquad \text{(i)} \qquad \beta(t) = \sum_{i=1}^{I} \beta_i(t) \qquad \text{(ii)} \qquad 14$$

$$\Lambda(t) = \frac{1}{\Gamma(t)} \int W \frac{1}{v} S \qquad 15$$

$$Q(t) = \int Wq \Big/ \int W \frac{1}{v} S \qquad 16$$

$$C_i(t) = \int W\chi_i c_i \Big/ \int W \frac{1}{v} S \qquad 17$$

which will be referred to as the point kinetics parameters.

Making these substitutions into equations (8) and (9) and rearranging gives:

$$\frac{\rho(t)-\beta(t)}{\Lambda(t)} T(t) + \sum_{i=1}^{I} \lambda_i C_i(t) + Q(t) = \frac{\delta T(t)}{\delta t} \int W \frac{1}{v} S + \frac{T(t)}{\Gamma(t)\Lambda(t)} \int W \frac{1}{v} \frac{\delta S}{\delta t} \qquad 18$$

$$\frac{\beta_i(t)}{\Lambda(t)} T(t) - \lambda_i C_i(t) = \frac{\delta C_i(t)}{\delta t} - \frac{1}{\Gamma(t)\Lambda(t)} \int \frac{\delta W}{\delta t} \chi_i c_i \qquad 19$$

Implementing the assumption of time independence of the weight and shape functions results in the standard form of the point kinetics equations:

$$\frac{\rho(t) - \beta(t)}{\Lambda(t)} T(t) + \sum_{i=1}^{I} \lambda_i C_i(t) + Q(t) = \frac{\delta T(t)}{\delta t} \qquad 20$$

$$\frac{\beta_i(t)}{\Lambda(t)} T(t) - \lambda_i C_i(t) = \frac{\delta C_i(t)}{\delta t} \qquad 21$$

This form of the equations is exact subject to the validity of the constraints which have been made. Given these assumptions are true, the application of the point kinetics equations to a transient problem is straight forward. Once a static or steady state flux shape has been determined, we simply apply the point kinetics equations along with the point kinetics parameters for the purpose of calculating the time dependent amplitude. The shape functions only use is then for the calculation of the kinetics parameters.

In general however, the shape changes at least slightly for a given perturbation in the system and there is some error built into the calculation of the point kinetics parameters. Since we do not wish to calculate this new shape function for all time, in order to satisfy the calculation of these parameters, we attempt to minimize the size of the error introduced by the error in the reference shape function by selecting a suitable weight function. How this weight function affects the calculation of the kinetics parameters and how it may minimize the error introduced by the choice of the shape function, can best be seen by making a quick study of the point kinetics parameters and their associated weight function.

The Weight Function

A very good discussion of the kinetics parameters is presented in Henry and we will only briefly discuss the aspects of the terms $\rho(t)$, $\Lambda(t)$ and $\beta_i(t)$ which play a role in the selection of a weight function.

First let us consider the term representing a weighted integral of the delayed neutron fraction $\beta_i(t)$.

$$\beta_i(t) = \frac{\int W \sum_j \chi_i \beta_i^j F^j S}{\int W \frac{1}{v} S} \qquad 22$$

The terms on the right hand side of this equation exhibiting time dependence are $W(r,E,t)$ and $F^j(r,E,t)S(r,E,t)$ which occur in both the numerator and denominator. Any variation in these values would therefore tend to cancel out and the parameter $\beta_i(t)$ ends up being only very slightly time dependent over the duration of a transient. This time dependence is in fact often ignored in practice leading to a negligible error in the results.

The second term to be considered is the parameter commonly referred to as the prompt neutron lifetime $\Lambda(t)$.

$$\Lambda(t) = \frac{1}{\Gamma(t)} \int W \frac{1}{v} S \qquad 23$$

Although the terms W and S both appear in the numerator and the denominator, the term F^j does not. This term is therefore not time independent for many transients and can cause significant error

in the final result if not accounted for. Variation in fission cross-section F^j however, is usually only slight in most transients and therefore the variation of $\Lambda(t)$ over portions of the transients may be very small and can be controlled via suitable choice of time steps. Therefore, from the point of view of selecting a weight function, this term does not provide much insight.

The last term to be considered is the parameter $\rho(t)$ commonly referred to as the reactivity.

24

$$\rho(t) = \frac{1}{\Gamma(t)} \int W(\nabla \cdot D \nabla S - AS + \sum_j (\chi_p^j (1-\beta^j) + \sum_{i=1}^{I} \chi_i \beta_i^j) F^j S)$$

The time dependence of this term occurs in both the numerator and the denominator, however its affect is more pronounced due to the diffusion and absorption terms in the numerator. We would therefore wish to choose a weight function W(r,E,t) such that any error in our choice of the static shape S(r,E,t), as the correct shape in the transient, be minimized in this parameter. In particular, since $\rho(t)$ is divided by $\Lambda(t)$ in the point kinetics equations, we would wish to minimize the contribution of the error in the numerator of R(t)

25

$$R(t) = \frac{\int W(\nabla \cdot D \nabla S - AS + \sum_j (\chi_p^j (1-\beta^j) + \sum_{i=1}^{I} \chi_i \beta_i^j) F^j S)}{\int W \frac{1}{v} S}$$

The term in the denominator is generally held constant over a time interval and any error here is controlled via time step selection. We will therefore concentrate only on the numerator of equation (25). Using a perturbation analysis approach, let's assume a small change in the steady state material properties resulting in a correspondingly small change in the shape function has occured. Therefore let:

$$A = A_o + \delta A \qquad \text{i}$$
$$F = F_o + \delta F \qquad \text{ii} \qquad 26$$
$$D = D_o + \delta D \qquad \text{iii}$$
$$S = S_o + \delta S \qquad \text{iv}$$

where D_o, A_o, F_o^j and S_o are the values at time zero. Making the substitution of equations (26) into the numerator of equation (25) results in:

$$R'(t) = \int W(\nabla\cdot D_o\nabla S_o + \nabla\cdot D_o\nabla\delta S + \nabla\cdot\delta D\nabla S_o + \nabla\cdot\delta D\nabla\delta S_o - A_oS_o - A_o\delta S - \delta AS_o \qquad 27$$
$$-\delta A\delta S + \sum_j(\chi_p^j(1-\beta^j) + \sum_{i=1}^{I}\chi_i\beta_i^j)(F_o^jS_o + F_o^j\delta S + \delta F_o^jS_o + \delta F_o^j\delta S_o))$$

noting that

$$\nabla\cdot D_o\nabla S_o - A_oS_o + \sum_j(\chi_p^j(1-\beta^j) + \sum_{i=1}^{I}\chi_i\beta_i^j)F_o^jS_o = 0 \qquad 28$$

and ignoring the terms in second order changes assuming they are small relative to terms in first order changes, we have

$$R'(t) = \int W(\nabla\cdot D_o\nabla\delta S + \nabla\cdot\delta D\delta S_o - A_o\delta S - \delta AS_o + \qquad 29$$
$$\sum_j(\chi_p^j(1-\beta^j) + \sum_{i=1}^{I}\chi_i\beta_i^j)(F_o^j\delta S + \delta F_o^jS_o))$$

The terms involving changes in material properties multiplied by the static flux shape can be interpreted as being those terms defining the change in reactivity due to changes in material properties relative to the steady state condition. Since these terms are generally known values, we wish to eliminate the terms involving the unknown value δS.

$$E = \int W(\nabla\cdot D_o\nabla\delta S - A_o\delta S - \sum_j(\chi_p^j(1-\beta^j) + \sum_{i=1}^{I}\chi_i\beta_i^j)F_o^j\delta S) \qquad 30$$

Rewriting the δS terms in equation (30) as $\delta S = S_o - S$ and noting equation (28) once again we have

$$E = \int W(\nabla \cdot D_o \nabla S - A_o S - \sum_j (\chi_p^j (1-\beta^j) + \sum_{i=1}^{I} \chi_i \beta_i^j) F_o^j S) \qquad 31$$

Expressing the operators A_o and F_o^j explicitly we have

$$E = \int W(\nabla \cdot D_o \nabla S - \Sigma_{to} S + \int_0^\infty dE' \Sigma_{so}(r,E' \to E,t) S(r,E',t) \qquad 32$$

$$- \int_0^\infty dE' \sum_j (\chi_p^j(E)(1-\beta^j) + \sum_{i=1}^{I} \chi_i(E) \beta_i^j) \nu \Sigma_{fo}(r,E',t) S(r,E',t))$$

Now since

$$\int_0^\infty dE\, W(r,E,t) \int_0^\infty dE' \Sigma_{so}(r,E' \to E,t) S(r,E,t)$$

$$= \int_0^\infty dE \int_0^\infty dE'\, W(r,E,t) \Sigma_{so}(r,E' \to E,t) S(r,E',t)$$

$$= \int_0^\infty dE' \int_0^\infty dE\, W(r,E',t) \Sigma_{so}(r,E \to E',t) S(r,E,t) \qquad 33$$

$$= \int_0^\infty dE\, S(r,E,t) \int_0^\infty dE' \Sigma_{so}(r,E \to E',t) W(r,E,t)$$

we can immediately interchange W and S in all terms in equation (32) except the one involving the diffusion coefficient. If we could equate

$$\int dV \int_0^\infty dE\, W(r,E,t) \nabla \cdot D_o(r,E,t) \nabla S(r,E,t) = \qquad 34$$

$$\int dV \int_0^\infty dE\, S(r,E,t) \nabla \cdot D_o(r,E,t) \nabla W(r,E,t)$$

then (32) could be written as

$$E = \int S(\nabla \cdot D_o \nabla W - \Sigma_{to} W + \int dE' \Sigma_{so}(r,E \to E',t) W(r,E',t)$$

$$+ \int dE' \sum_j (\chi_p^j (1-\beta^j) + \sum_{i=1}^{I} \chi_i(E) \beta_i^j) \nu \Sigma_{fo}(r,E') W(r,E',t)) \qquad 35$$

If we could choose the weight function so that the term multiplied by S inside the integral disappears, we would eliminate the major source of first order errors in the reactivity calculation due to the choice of the shape function. Therefore equating this term to zero, we have:

$$\nabla \cdot D_o \nabla W - A_o^T W + \sum_j (\chi_p^j (1-\beta^j) + \sum_{i=1}^{I} \chi_i \beta_i^j) F_o^j W = 0 \qquad 36$$

where A_o^T is equivalent to the operator A_o with the directional dependence of the scattering and fission terms transposed. This equation is very similar to the static flux equation and shares the same boundary conditions and is defined over the same time, space and energy domain as the shape function. The solution of this equation then fulfills all of the all of the requirements of a weight function and even though equation (34) is generally not exactly satisfied, it is still a good choice for the weight function. This function, the adjoint function, has been universally accepted as the appropriate weight function in the point kinetics equations. We note at this time that should $W(r,E,t) = S(r,E,t)$ that equation (34) would hold exactly true and our problem would be self adjoint. This fact will support our development in later stages.

The choice of the adjoint function as our weight function presents us with several complications with respect to application. Firstly, we now require the calculation of a second steady state solution, in addition to the steady state flux calculation. It also requires the storage of this vector, equal in size to the shape function. Further we note, that since the steady state time independent adjoint function has historically been used as the weight function, its dependence on the material properties of the system being exactly the same as the flux shape function, leads to errors in the kinetics parameters calculation in the same way as the choice of the static flux shape. Therefore we conclude that the use of the

static adjoint in the point kinetics calculations would only be valid for transients in which the static flux shape is also a good choice.

Other choices for the adjoint function have not been eliminated because of the discovery of the adjoint function. Although a constant weight function such as the value 1.0 would not be an ideal choice for a weight function we can see that results using this value would be perfectly valid if our shape function were to remain constant. Analytical weight functions may also be used to approximate the adjoint depending on how critical an error in weight function may be in the solution of the problem. The possible magnitude of error associated with an incorrect choice of weight function is well illustrated by Martin Becker[6] in his discussion concerning the desireability of a time dependent adjoint function versus the static adjoint weight function. In thermal reactors particularly the final shape of the neutron flux after a disturbance in the system may be quite different from the original shape. Although this shape change may occur showly over a period of time, one has to question the validity of using a time independent adjoint shape in the calculation of the kinetics parameters. A phenomena known as flux tilt in Candu reactors where the amplitude of the local flux may be much greater in one half of the reactor compared with the corresponding point in the other half, is just one such situation. A methodology for applying a time dependent weighting function to a transient analysis will be demonstrated during our development of the I.Q.S. method on which we will base our scheme.

The Improved QuasiStatic Approximation (I.Q.S.)

The I.Q.S. method is an iterative numerical solution method for the reactor kinetics problem which has evolved from a method known as the QuasiStatic Approximation. The differences between these two methods and an earlier relative known as the Adiabatic Approximation are described in a paper by K.O. Ott and D.A. Meneley[3]. All three of these methods provide a means of coupling the shape function calculations to the point kinetics equations in problems where significant changes in flux shape are expected. To see how this is accomplished, we will begin by developing the appropriate shape and precursor equations to be used in conjunction with the point kinetics equations.

Returning to equations (1) and (2) and substituting relationship (6) gives us the equations

$$T(t)\nabla\cdot D\nabla S - T(t)AS + T(t)\sum_j \chi_p^j (1-\beta^j) F^j S + \sum_{i=1}^{I} \chi_i \beta_i c_i + q \qquad 37$$

$$= \frac{1}{v}\left(\frac{\delta T(t)}{\delta t} S + T(t)\frac{\delta S}{\delta t}\right)$$

$$T(t)\sum_j \chi_i^j F^j S - \lambda_i c_i = \frac{\delta c_i}{\delta t} \qquad 38$$

Dividing equation (37) through by T(t) and rearranging terms gives us a useable form of the shape function

$$\nabla\cdot D\nabla S + \left(-A + \sum_j \chi_p^i (1-\beta^j) F^j - \frac{1}{v}\frac{\dot{T}(t)}{T(t)}\right) S + \frac{1}{T(t)} \sum_{i=1}^{I} \chi_i \lambda_i c_i \qquad 39$$

$$+q/T(t) = \frac{1}{v}\frac{\delta S}{\delta t}$$

where changes in the shape function are assumed to be linear in any time interval.

The spacial precursor equations are integrated formally to obtain:

$$c_i(t) = c_i(0)\mathrm{Exp}(-\lambda_i t) + \int_0^t \sum_j \beta_i^j F^j T(\tau)\mathrm{Exp}(-\lambda_i(t-\tau))S d\tau \qquad 40$$

These two equations plus the point kinetics equations and the associated kinetics parameters form the complete set of equations used in the I.Q.S. method. In solving these equations over a transient time step, we treat them as a pair of coupled equations with equation (39) as the first member of the pair and equations (40) along with the point kinetics equations as the second member of the pair. Having obtained a steady state solution to the problem and the static adjoint solution to the same problem, we initiate a transient by making some known change in the material configuration of the reactor. We then begin the transient analysis by defining a time period over which we expect the point kinetics to hold approximately true, this being a time period over which the shape change is small. This can be determined by examining the effect of the change on the reactor reactivity or simply by implementing a suitably small time step and allowing certain tests to determine the validity of this time step and size of further time steps. We next integrate the point kinetics equations in a step wise fashion over the time step to solve for the amplitude function. An algorithm presented by J.J. Kaganove[7] can be applied for this purpose. The precursor equations (40) are also integrated along with the kinetics equations using the values from the amplitude integration until we reach the end point of the prescribed time interval for shape function calculation. Equation (39) is now solved using the results of the point kinetics and precursor equations. Once this has been completed, the validity of equation (11) over the interval is tested and the next time step is chosen. The solution then proceeds in the same fashion over the next interval.

Should our problem be self adjoint making it possible to replace the steady state adjoint function with a properly normalized shape function this algorithm suggests a simple application of a time dependent weight function. Some extra terms will appear in the point kinetics calculations which complicate the matter but the sequence of solution would remain unchanged. With the property of self adjointness then the present shape function would replace the old weight function during calculations over the next time period. The validity and advantages of a self adjointness assumption and application will be discussed in the next section.

The Self-Adjointness Assumption

As we have pointed out in our search for an appropriate weight function and our discussion of the I.Q.S. method, self adjointness would not only give us a better weight function, but could also be easily implemented in the I.Q.S. scheme. It would also alleviate the problems presented by Becker with respect to a time dependent weighting scheme. Before looking for properties of self adjointness in the Candu context, lets discuss the validity of time dependent weighting.

Given any reactor transient initiated at time t, in which a large change in flux shape was expected, we will try to visualize a material system in which the present transient flux shape is the steady state condition. If this steady state was the starting point of our transient, rather than some intermediate point, we could initiate material changes which would follow exactly the route of the transient presently under study. On the premise that shape changes occur quickly with respect to the rate of change of material properties, the material configuration resulting in our hypothetical intermediate steady state would differ only slightly from the material properties present at the time during the transient leading to the flux shape in question. We therefore conclude, that the appropriate adjoint weighting function at this time would be that of the steady state configuration rather than the weight function derived from some steady configuration at the onset of the transient. If our problem were indeed self adjoint, this adjoint weighting function would then closely follow the present flux shape. Remembering the development leading to the choice of the adjoint function as weight function, consider the implications of a small error in $W(r,E,t)$ because of a choice of the present flux shape in the self adjoint system, versus the larger error introduced due to the choice of the time zero static

adjoint weight function. We would expect the present value to give much better results in a near self adjoint system than the time zero value.

A simple way to look for self adjointness properties in a system is to compare the static flux shape with the static adjoint for the same material configuration. Just such a comparison has been made in the test cases of Appendix A of this report. By visually comparing the shapes of the two functions for different material configurations we can see that the self adjointness property holds better for some material configurations than for others. A statistical comparison of the point by point ratios of the flux shapes to the adjoint shapes, gives us further insight to the closeness of a self adjointness assumption. The worst results occur for the configuration having large reflector regions while the best non self adjoint configuration is that one having only one material region. Large present day reactors tend to have macroscopically homogeneous cores making the single region shape look promising but the presence of control rods used to flatten the flux shape within the reactor presents us with a multiregion system such as present in case number 1. This case is more radical than those expected in the Candu but does provide a good test of the self adjointness assumption.

The One Dimensional Diffusion Code

To test the proposed algorithm, we have chosen to write a one dimensional diffusion code in slab configuration. The code is designed to solve the two group neutron diffusion equations with six delayed neutron precursor groups and will be capable of solving the steady state flux shape and the steady adjoint flux shape. It will also be able to run transient test cases using the I.Q.S. method with constant weighting, steady state adjoint weighting and variations of the self weighting scheme.

Numerical schemes for solving the multigroup diffusion equation are prevalent throughout the literature. The scheme we have adopted follows that outlined by G.K. Leaf and A.S. Kennedy[8]. Only the finite difference equations in slab configuration will be developed here.

The steady state equation equivalent to equation (1) in multigroup form can be written

$$-\nabla \cdot D_g \nabla \phi_g + \sigma^R_g \phi_g = S_g \qquad 41$$

where the subscript g is the energy group identifier. For the two group case, it will have a value of 1 for the fast flux group and 2 for the thermal flux group. S_g represents the fission and scattering group source terms.

In slab configuration, we can express the first term of equation (41) as

$$\nabla \cdot D_g \nabla \phi_g = \frac{d}{dr}\left(D_g(r) \frac{d\phi_g}{dr}\right) \qquad 42$$

By dividing the slab into intervals R_{i-1}, R_i where i=1,2,3...I and $0=R_o < R_1 < R_2 .. < R_I = R$ as in figure (1),

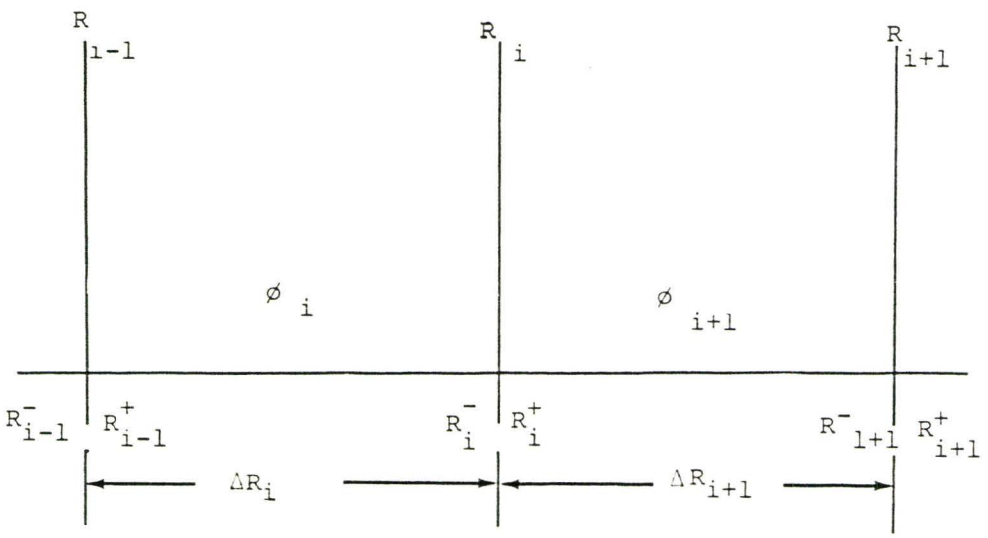

Figure 1

we can integrate the equation over an interval assuming constant crossections and diffusion coefficient giving

$$\int_{R_{i-1}^{+}}^{R_i^{-}} \frac{d}{dr}\left(D(r)\frac{d\phi(r)_g}{dr}\right)dr + \int_{R_{i-1}^{+}}^{R_i^{-}} \sigma_g^R \phi_g(r)\,dr = \int_{R_{i-1}^{+}}^{R_i^{-}} S_g\,dr \qquad 43$$

If we make the approximation that

$$\int_{R_{i-1}^{+}}^{R_i^{-}} \phi_g(r)\,dr \simeq \phi_g(r_i)V_i \qquad 44$$

where $\phi_g(r_i)$ is the average flux value within the interval and is assumed to reside at the midpoint of the interval. Now adopting the notation

$$\phi_{gi} = \phi_g(r_i) \qquad \text{where} \qquad r_i = \frac{R_i^{-} + R_{i+1}^{+}}{2} \qquad 45$$

and noting that in slab configuration an incremental volume $V_i = \Delta R_i$ we have

$$D_g(r_i)\frac{d\phi(r)}{dr}\Bigg|_{R_{i-1}^{+}}^{R_i^{-}} + \sigma_{gi}^R \phi_{gi}\Delta R_i = S_{gi}\Delta R_i \qquad 46$$

or

$$D_g(r_i)(\phi'(R_i^{-}) - \phi'(R_{i-1}^{+})) + \sigma_{gi}^R \phi_i \Delta R_i = S_{gi}\Delta R_i \qquad 47$$

Now considering Taylor's Theorem of the mean

$$f(x_o+h) = \frac{f(x_o)}{0!} + \frac{hf'(x_o)}{1!} + \frac{h^2 f''(x_o)}{2!} + \ldots\ldots \qquad 48$$

and letting the group subscript be left as understood, we can write the flux term at R_i as

$$\phi(R_i^-) = \phi_i + \frac{\Delta R_i}{2}\phi_i' + \frac{\Delta R_i^2}{4}\frac{\phi_i''}{2!} + \frac{\Delta R_i^3}{8}\frac{\phi_i'''}{3!} + \ldots\ldots \qquad 49$$

Similarly the flux term at R_i can be expressed in terms of the flux in the next interval as

$$\phi(R_i^+) = \phi_{i+1} - \frac{\Delta R_{i+1}}{2}\phi_{i+1}' + \frac{\Delta R_{i+1}^2}{4}\frac{\phi_{i+1}''}{2!} - \frac{\Delta R_{i+1}^3}{8}\frac{\phi_{i+1}'''}{3!} + \ldots. \qquad 50$$

Now by taking the derivatives of these two equations, we have

$$\phi'(R_i^-) = \phi_i' + \frac{\Delta R_i}{2}\phi_i'' + \frac{\Delta R_i^2}{4}\frac{\phi_i'''}{2!} + \frac{\Delta R_i^3}{8}\frac{\phi_i''''}{3!} + \ldots\ldots \qquad 51$$

$$\phi'(R_i^+) = \phi_{i+1}' - \frac{\Delta R_{i+1}}{2}\phi_{i+1}'' + \frac{\Delta R_{i+1}^2}{4}\frac{\phi_{i+1}'''}{2!} - \frac{\Delta R_{i+1}^3}{8}\frac{\phi_{i+1}''''}{3!} + \ldots. \qquad 52$$

Substitution of ϕ_i and ϕ_{i+i} from these two equations, into (49) and (50) gives

$$\phi(R_i^-) = \phi_i + \frac{\Delta R_i}{2}(\phi'(R_i^-) - \frac{\Delta R_i}{2}\phi_i'' - \frac{\Delta R_i^2}{4}\frac{\phi_i'''}{2!} - \ldots.) + \frac{\Delta R_i^2}{4}\frac{\phi_i''}{2!} + \ldots. \qquad 53$$

and

$$\phi(R_i^+) = \phi_{i+1} - \frac{\Delta R_{i+1}}{2}(\phi'(R_i^+) + \frac{\Delta R_{i+1}}{2}\frac{\phi_{i+1}''}{1!} - \frac{\Delta R_i^2}{4}\frac{\phi_{i+1}'''}{2!} + \ldots.) + \frac{\Delta R_i^2}{4}\frac{\phi_{i+1}''}{2!} - \ldots. \qquad 54$$

Multiplying equation (53) by $\Delta R_{i+1} D_i$ and (54) by $\Delta R_i D_{i+1}$ adding and ignoring terms of order higher than ϕ' we have

$$\Delta R_{i+1} D_i \phi(R_i^-) + \Delta R_i D_{i+1} \phi(R_i^+) = \qquad 55$$

$$\Delta R_{i+1} D_i \phi_i + \Delta R_i D_{i+1} \phi_{i+1} + \frac{\Delta R_{i+1} \Delta R_i}{2} (D_i \phi'(R_i^-) - D_{i+1} \phi'(R_i^+))$$

By continuity of current requirements and continuity of flux at boundaries

$$D_i \phi'(R_i^-) = D_{i+1} \phi'(R_i^+) \quad \text{and} \quad \phi(R_i^-) = \phi(R_i^+) = \phi(R_i) \qquad 56$$

we have

$$(\Delta R_{i+1} D_i + \Delta R_i D_{i+1}) \phi(R_i) = \Delta R_{i+1} D_i \phi_i + \Delta R_i D_{i+1} \phi_{i+1} \qquad 57$$

and therefore

$$\phi(R_i) = \frac{\Delta R_{i+1} D_i \phi_i + \Delta R_i D_{i+1} \phi_{i+1}}{\Delta R_{i+1} D_i + \Delta R_i D_{i+1}} \qquad 58$$

Substituting this equation back into equation (53) again ignoring terms of order higher than ϕ' gives

$$D_i \phi'(R_i^-) = \frac{-2D_i}{\Delta R_i} \left(\phi_i - \frac{\Delta R_{i+1} D_i \phi_i + \Delta R_i D_{i+1} \phi_{i+1}}{\Delta R_{i+1} D_i + \Delta R_i D_{i+1}} \right) \qquad 59$$

and by a similar development

$$D_i \phi'(R_{i-1}^+) = \frac{2D_i}{\Delta R_i} \left(\phi_i - \frac{\Delta R_i D_{i-1} \phi_{i-1} + \Delta R_{i-1} D_i \phi_i}{\Delta R_i D_{i-1} + \Delta R_{i-1} D_i} \right) \qquad 60$$

Substituting (59) and (60) into equation (47)

$$(\sigma^R \Delta R_i + \frac{2D_i}{\Delta R_i}(1-\frac{\Delta R_{i+1} D_i}{\Delta R_{i+1} D_i + \Delta R_i D_{i+1}}) + \frac{2D_i}{\Delta R_{i-1}}(1-\frac{\Delta R_{i-1} D_i}{\Delta R_i D_{i-1} + \Delta R_{i-1} D_i})) \phi_i$$

$$-\frac{2D_i}{R_i}(\frac{\Delta R_i D_{i+1}}{\Delta R_{i+1} D_i + \Delta R_i D_{i+1}}) \phi_{i+1} \quad -\frac{2D_i}{\Delta R_{i-1}}(\frac{\Delta R_i D_{i-1}}{\Delta R_i D_{i-1} + \Delta R_{i-1} D_i}) \phi_{i-1} = S_i \Delta R_i \qquad 61$$

defining terms

$$a_i = \frac{2D_i D_{i+1}}{\Delta R_{i+1} D_i + \Delta R_i D_{i+1}} \qquad \text{i}$$

$$c_i = \frac{2D_i D_{i-1}}{\Delta R_i D_{i-1} + \Delta R_{i-1} D_i} \qquad \text{ii} \qquad 62$$

$$e_i = \sigma^R R_i + a_i + c_i \qquad \text{iii}$$

giving us the finite difference form of the two group neutron diffusion equation

$$-c_i \phi_{i-1} + e_i \phi_i - a_i \phi_{i+1} = S_i \Delta R_i \qquad 63$$

Conditions at the external boundaries of the problem can be expressed as

$$A\phi'(R) + B\phi(R) = C \qquad 64$$

where A, B and C are group dependent parameters. The usual assumption is that the source term C is zero at the boundary and the flux term $\phi(R)$ is equal to zero at some extrapolated distance from the boundary. The resulting boundary conditions then are, for the left hand side

$$c_1 = 0 \qquad \text{i}$$

$$e_1 = a_1 + \sigma^R \Delta R_1 + \frac{D_1 B}{A + \frac{1}{2}\Delta R_1 B} \qquad \text{ii} \qquad 65$$

and for the right hand side

$$a_I = 0 \qquad i$$

$$e_I = c_I + \sigma^R \Delta R_I + \frac{D_I \mathcal{B}}{A + \frac{1}{2} R_I \mathcal{B}} \qquad ii \qquad 66$$

Our finite difference equations can then be written as

$$-a_{ig}\phi_{i+1,g} + e_{ig}\phi_{ig} - c_{ig}\phi_{i-1,g} = \qquad 67$$

$$\sum_{g' \neq g}^{G} \Delta R_i \sigma^{g' \to g} \phi_{g'} + \frac{1}{k} \sum_{g'=1}^{G} \Delta R_i \chi_i^{g' \to g} \nu\sigma_{fi,g'} \phi_{ig'}$$

where we have expanded the source term into its scattering and fission components respectively. With external boundary conditions of the form

$$A_g \frac{\delta \phi_g}{\delta r} + \mathcal{B}_g \phi_g = 0 \qquad 68$$

we have the complete homogenous finite difference equations to be solved.

Solution of the Finite Difference Equations

Rewriting equation (67) in matrix form we have

$$M_g \phi_g = \sum_{g' \neq g}^{G} B^{g' \to g} \phi_g + \frac{1}{k} \sum_{g'=1}^{G} F^{g' \to g} \phi_{g'} \qquad 69$$

where

$$M_g = \begin{vmatrix} e_{1,g} & -a_{1,g} & & & & & \\ -c_{2,g} & e_{2,g} & -a_{2,g} & & & & \\ & -c_{3,g} & e_{3,g} & -a_{3,g} & & & \\ & & \cdot & \cdot & \cdot & & \\ & & & \cdot & \cdot & \cdot & \\ & & & -c_{I-1,g} & e_{I-1,g} & -a_{I-1,g} & \\ & & & & -c_{I,g} & e_{I,g} & \end{vmatrix} \quad i \qquad 70$$

for $g = 1,2,.....G$

$$B^{g' \to g} = \text{diag}(\Delta R_i \sigma_i^{g' \to g}) \qquad ii$$

$$F^{g' \to g} = \text{diag}(\chi_i^{g' \to g} \sigma_{fi,g} \Delta R_i) \qquad iii$$

where we have assumed all fissions produce neutrons in only one group. The fast neutron group. We will also assume from this point on that only downscattering occurs and the probability of upscatter is therefore zero.

Considering only a two group model, we can further simplify equation (69) by defining matrices

$$E = \begin{vmatrix} M_1 & 0 \\ -B^{1 \to 2} & M_2 \end{vmatrix} \qquad F = \begin{vmatrix} F^{1 \to 1} & F^{2 \to 1} \\ 0 & 0 \end{vmatrix} \qquad 71$$

giving

$$E\phi = \frac{1}{k} F\phi \qquad 72$$

As a solution to equation (72) we seek a positive vector ϕ, since negative flux is a nonphysical quantity, corresponding to the largest k eigenvalue. This search is carried out iteratively using a power iteration method on the matrix $E^{-1}F$. Starting with an arbitrary positive flux guess $\phi^{(o)}$ and a positive $k^{(o)}$ we iteratively form

$$E\phi^{(n+1)} = \frac{1}{k^{(n)}} F\phi^{(n)} \quad \text{where} \quad k^{(n+1)} = k^{(n)} \frac{<\phi^{(n+1)}, \phi^{(n+1)}>}{<\phi^{(n+1)}, \phi^{(n)}>} \qquad 73$$

Inner iterations of $\phi^{(n+1)}$ will be solved using a Guass-Seidel iterative scheme, with the outer iteration solving for the new value of $k^{(n+1)}$. The system is said to have converged when

$$|k^{(n+1)} - k^{(n)}| < \xi_k \qquad 74$$

and

$$\frac{\sum_{g=1}^{2} \sum_{i=1}^{I} |\phi_{i,g}^{(n+1)} - \phi_{i,g}^{(n)}|}{\sum_{g=1}^{2} \sum_{i=1}^{I} |\phi_{i,g}^{(n+1)} * \phi_{i,g}^{(n+1)}|} < \xi_\phi \qquad 75$$

Both of these tests are not necessary as the $k^{(n+1)}$ iterates tend to converge before the inner $\phi_{i,g}^{(n+1)}$ iterates.

The steady state adjoint equation can be found in a similar manner simply by transposing the E and F matrices and solving as for the steady state flux equation.

The Transient Algorithm

Having established the steady state solution of the finite difference form of the group neutron diffusion equations and the adjoint equation if desired, we initialize the transient finite difference coefficients by dividing the fission matrix through by $k_{eff}=k^{(n+1)}$ where n signifies the last outer iteration. This will establish a steady state material system from which to initiate our transient. Our fission matrix then becomes

$$F^{g'\rightarrow g} = \text{diag}(\chi^{g}_{ik}\frac{\nu}{k_{eff}}\sigma_{fg,i}\Delta R_i) \qquad 76$$

The next step is to normalize the flux vector and weight functions according to equation (11) such that

$$\sum_{i=1}^{N}\Delta R_i\sum_{g=1}^{2}W^{o}_{g,i}\frac{1}{v}S^{o}_{g,i} = 1.0 \qquad 77$$

where we have arbitratily chosen $S^{o}_{gi}=\phi^{o}_{gi}$ and normalized the weight function to satisfy equation (77). From this time onwards the weight function will remain unchanged in the transient except in the case of self weighting scheme where we apply equation (77) at the beginning of every time step. This choice of weighting scheme normalization naturally leads to a choice of the time zero amplitude as

$$T(t_o) = \phi^{o}_{g,i}/S^{o}_{g,i} \qquad 78$$

Having established our shape function, we can now initialize the steady state precursor density matrices as

$$P(i,j) = \frac{1}{\lambda_j} \text{diag}\left(\sum_{g=1}^{2} \beta_j \chi_j^g \nu\phi_{fg,i} \frac{\Delta R_i S_{g,i}}{k_{eff}} \right) \qquad 79$$

followed by the time zero calculation of the point kinetics parameters, equations (10) through (15). This completes all of the input requirements for the transient algorithm. The next step is to initiate some change in the material properties.

As outlined in the description of the I.Q.S. method, the complete set of transient equations consists of the shape function equations along with the integrated precursor equations, point kinetics equations and associated kinetics parameters. We will denote time points at which the shape function is to be solved as the t^m time points and the time interval t^m to t^{m+1} as the Δt^m iteration interval. Time points at which the precursors and point kinetics equations are to be integrated will be designated as t^n time points and the interval from t^n to t^{n+1} as the Δt^n interval. The time step sequence will then be to solve the shape function at time t^m followed by the integration of the point kinetics equations and the precursor equations at intervals Δt^n up to time t^{m+1} where the next shape function iterations occur, using the results of the Δt^n time steps. Let's first turn our attention towards the integration of the precursor equations on the interval t^n, t^{n+1}.

Integrating equation (38) formally over the interval gives the relationship

$$c_i^{(n+1)} = c_i^{(n)} \exp(-\lambda_i (t^{n+1}-t^n)) + \int_{t^n}^{t^{n+1}} F^{g' \to g} T(t) \exp(-\lambda_i (t^{n+1}-t)) S(t) dt \qquad 80$$

Now assuming a linear relationship for $F^{g \to g}S(t)$ in the interval gives

$$c_i^{(n+1)} = c_i^{(n)} \exp(-\lambda \Delta t^n) + a_i^n (F^{g' \to g} S(t^{n+1})) + b_i^n (F^{g' \to g} S(t^n)) \quad 81$$

where

$$a_i^n = \frac{1}{\Delta t^n} \int_{t^n}^{t^{n+1}} \exp(-\lambda (t^{n+1} - t))(t - t^n) T(t) dt \quad i \quad 82$$

$$b_i^n = \int_{t^n}^{t^{n+1}} \exp(-\lambda (t^{n+1} - t)) T(t) dt - a_i^n \quad ii$$

We now need only have a relationship for T(t) over the interval to solve for the values a^n and b^n. Returning to the derived form of the point kinetics equations, equations (16) and (17) we have

$$\frac{\rho(t) - \beta(t)}{\Lambda(t)} T(t) + \sum_{i=1}^{I} \lambda_i c_i(t) + Q(t) = \frac{\delta T(t)}{\delta t} \int W \frac{1}{v} S + \frac{T(t)}{\Gamma(t)\Lambda(t)} \int W \frac{1}{v} \frac{\delta S}{\delta t} \quad 83$$

and

$$\frac{\beta_i(t)}{\Lambda(t)} T(t) - \lambda_i C_i(t) = \frac{\delta C_i(t)}{\delta t} - \frac{1}{\Gamma(t)\Lambda(t)} \int \frac{\delta W}{\delta t} \chi_i c_i(t) \quad 84$$

We can rearrange equation (83) to give

$$\left(\frac{\rho(t) - \frac{1}{\Gamma(t)} \int W \frac{1}{v} \frac{\delta S}{\delta t}}{(t)} \right) T(t) - \sum_{i=1}^{I} \frac{\delta C_i(t)}{\delta t} + Q(t) = \frac{\delta T(t)}{\delta t} \quad 85$$

Since the time dependence of $\beta_i(t)$ is usually very small throughout the transient and similarly the variation of $\Lambda(t)$ is small over a time step, and time steps can be chosen to ensure this, we will

neglect the time dependence of these two variables over a transient time period Δt^m. We can then integrate equation (84) over an interval Δt^n giving

$$C_i(t^{n+1}) - C_i(t^n) = -C_i(t^n)(1-\exp(-\lambda_i \Delta t^n)) + \frac{\beta_i}{\Lambda}\int_{t^n}^{t^{n+1}} \exp(-\lambda_i(t^{n+1}-t))T(t)dt + \int_{t^n}^{t^{n+1}} \frac{1}{\Gamma(t)\Lambda}\int \frac{\delta W}{\delta t}\chi_i c_i dV dt \qquad 86$$

and also integrate equation (85) term by term to give

$$T(t^{n+1}) - T(t^n) = \int_{t^n}^{t^{n+1}} \frac{R(t)}{\Lambda} T(t) - \sum_{i=1}^{I}(C_i(t^{n+1}) - C_i(t^n)) + \int_{t^n}^{t^{n+1}} Q(t) \qquad 87$$

where $R(t) = (\rho(t) - \frac{1}{\Gamma(t)}\int W \frac{1}{v}\frac{S}{t})/\Lambda$

and assume over the interval that

$$R(t) = R_o + R_1(t-t^n) + R_2(t-t^n)^2 \qquad \text{i}$$

$$T(t) = T_o + T_1(t-t^n) + T_2(t-t^n)^2 \qquad \text{ii}$$

$$\frac{\delta W}{\delta t} = \frac{W(t^{m+1}) - W(t^m)}{\Delta t^m} \qquad 88 \text{ iii}$$

$$c_i(t) = c_i(t^n) + \frac{c_i(t^{n+1}) - c_i(t^n)}{\Delta t^n}(t-t^n) \qquad \text{iv}$$

The resulting equation then becomes

$$T_1(\Delta t^n)+T_2(\Delta t^n)^2=\frac{1}{\Lambda}\int_{t^n}^{t^{n+1}}(R_o+R_1(t-t^n)+R_2(t-t^n)^2)(T_o+T_1(t-t^n)+$$

$$T_2(t-t^n)^2) - \sum_{i=1}^{I}(-C(t^n)(1-\exp(-\lambda_i\Delta t^n)+\frac{\beta_i}{\Lambda}\int_{t^n}^{t^{n+1}}\exp(-\lambda_i(t^{n+1}-t)(T_o+ \quad (89)$$

$$T_1(t-t^n)+T_2(t-t^n)^2)+\frac{1}{\Gamma\Lambda}\int_{t^n}^{t^{n+1}}((T_o+T_1(t-t^n)+T_2(t-t^n)^2)*$$

$$\int dV\frac{W(t^{m+1})-W(t^m)}{\Delta t^m}(c_i(t^n)+\frac{c_i(t^{n+1})-c_i(t^n)}{\Delta t^n}(t-t^n)))$$

Now by defining

$$I_{i,m} = \frac{1}{\Delta t^{m+1}}\int_{t^n}^{t^{n+1}}\exp(-\lambda_i(t^{n+1}-t))(t^{n+1}-t)^m dt \quad (90)$$

and collecting terms in T_1, T_2 and T_o we have the result

$$T_1(1-\Delta t^n(\frac{R_o}{2}+\frac{R_1\Delta t^n}{3}+\frac{R_2(\Delta t^n)^2}{4} - \sum_{i=1}^{I}(\frac{\beta_i}{\Lambda}I_{i,1}))) +$$

$$T_2(1-(\Delta t^n)^2(\frac{R_o}{3}+\frac{R_1\Delta t^n}{4}+\frac{R_2(\Delta t^n)^2}{5} - \sum_{i=1}^{I}(\frac{\beta_i}{\Lambda}I_{i,2}))) = \quad (91)$$

$$(T_o(R_o+\frac{R_1\Delta t^n}{2}+\frac{R_2(\Delta t^n)^2}{3}) + \sum_{i=1}^{I}C_i(t^n)(1-I_{i,0}) - \sum_{i=1}^{I}T_o\frac{\beta_i}{\Lambda}I_{i,0}$$

$$- \sum_{i=1}^{I}(T_o\frac{\Delta W}{\Delta t}C_i(t^n)I_{i,0} + T_o\frac{\Delta W}{\Delta t}\frac{\Delta C_i}{\Delta t}I_{i,1}))$$

where

$$\frac{\Delta W}{\Delta t}C_i(t^n) = \frac{1}{\Gamma\Lambda}\int\frac{W(t^{m+1}) - W(t^m)}{\Delta t^m}\chi_i c_i(t^n)dV \quad (92)$$

and

$$\frac{\Delta W}{\Delta t}\frac{\Delta C}{\Delta t} = \frac{1}{\Gamma\Lambda}\int\frac{W(t^{m+1}) - W(t^m)}{\Delta t^m}\chi_i\frac{c_i(t^{n+1}) - c_i(t^n)}{\Delta t^n}dV \quad (93)$$

Substituting equation (88,ii) into equation (85) gives us

$$C_i(t^{n+1}) = C_i(t^n) + \frac{\beta_i}{\Lambda}(T_o I_{i,0} + T_1 I_{i,1} + T_2 I_{i,2}) \qquad 94$$

$$+ \frac{\Delta W}{\Delta t} C_i(t^n) I_{i,0} + \frac{\Delta W}{\Delta t}\frac{\Delta C}{\Delta t} I_{i,1}$$

as our integrated precursor density equation. Through a similar development we define equations equivalent to (91) at the half time interval $\Delta t^n/2$ and the quarter time interval $\Delta t^n/4$. This results in two sets of equations of two equations and two unknowns, the first set being the equations at the full time interval Δt^n and the half time interval $\Delta t^n/2$ and the second set being the equations at the half and quarter intervals. Since both sets of equations would ideally give us the same result for T_1 and T_2 but in practice do not, we can define an interval error

$$E(t^n) = \left| \frac{T_1(\Delta t^n) + \frac{1}{2} T_2(\Delta t^n)}{T_1(\frac{\Delta t^n}{2}) + \frac{1}{2} T_2(\frac{\Delta t^n}{2})} \right| \qquad 95$$

and prescribe error bounds $_1$ and $_2$ to control the Δt^n interval sizes as follows

$$\text{i} \quad \xi_1 \ll E(\Delta t^n) \ll \xi_2$$

Maintain the current interval size in the next integration step

$$\text{ii} \quad E(\Delta t^n) < \xi_1 < \xi_2$$

The present step size is too small and the next step size will be two times the present value.

iii $\xi_1 < \xi_2 < E(\Delta t^n)$

The present step size is too large and the interval step size will be divided by two and the integration step repeated with the smaller step size.

Once an integration interval has been accepted, the precursor equations (81) and (82) can be updated. We now repeat the integration over the next interval until time t^{m+1} is reached.

At this time we return to equation (37) written in matrix form as

96

$$ES = F^{g'\to g}S + \frac{1}{T(t)}\sum_{j=1}^{6}\chi_j\beta_j P(i,j) - \frac{1}{v}\frac{\dot{T}(t)}{T(t)} + \frac{q}{T(t)} - \frac{1}{v}\frac{\delta S}{\delta t}$$

where

$$\frac{1}{v} = \text{diag}\left(\frac{1}{v_g}\right)$$

Assuming that the shape function varies in a linear fashion with time as in the point kinetics equations just developed and lumping, the external and delayed neutron sources into a matrix Q we can write

97

$$\left[\frac{1}{v}\left(\frac{1}{\Delta t^m} + \frac{T(t^m)}{T(t)}\right) + E^m\right]S(t^m) = F^{g'\to g}S(t^{m-1}) + Q(t^m)$$

where

$$-\frac{1}{v}\frac{\delta S}{\delta t} = -\frac{1}{v}\frac{S(t^m) - S(t^{m-1})}{\Delta t^m} \qquad i \qquad 98$$

$$Q(t^m) = \frac{1}{T(t^m)}\left[\sum_{j=1}^{6}\chi_j^d\lambda_j P(i,j,t^m) + q(t^m)\right] + \frac{1}{\Delta t^m}\frac{1}{v}S(t^{m-1})$$

Equation (97) can then be solved for $S(t^m)$ using a source iteration technique. To accelerate convergence the normalization

$$k^n = \langle W \frac{1}{v} S \rangle = \sum_{i=1}^{N} \Delta R_i \sum_{g=1}^{2} W_{g,i}^{m-1} \frac{1}{v_g} S_{g,i}^{m} \qquad 99$$

is implemented as in the steady state iterations to give

$$\left[\frac{1}{v} \left(\frac{1}{t^m} + \frac{\dot{T}(t^m)}{T(t^m)} \right) + E^m \right] S^n(t^m) = \frac{F^{g' g}}{k^m} S^{n-1}(t^m) + Q(t^m) \qquad 100$$

as the equation being solved. Once our new shape function has been found, the validity of the time step Δt^m and the choice of Δt^{m+1} must be determined.

This then constitutes the complete set of transient equations necessary to solve any transient problem using either constant or transient weighting functions. In the case of the constant adjoint function or constant weighting schemes, the extra terms in the point kinetics integration scheme become zero and pose no calculational problems. For the transient adjoint weighting scheme, the weight function and precursor density function derivatives in the time interval t^m must be approximated. This can be done by assuming the values from the t^{m-1} interval in the t^m interval or using a new best guess by recalculating these values at the end of each t^m iteration before proceeding to the next t^{m+1} level.

The Δt^m iteration level is said to have converged when

$$\left| \frac{R(t^{m+1}) - R^*(t^{m+1})}{R(t^{m+1})} \right| < \xi_\rho \qquad 101$$

where the * signifies the previous gues for this value. The shape function and point kinetics functions are then recalculated from time t^m to t^{m+1} until this criteria is satisfied or a maximum number of iterations has occurred before proceeding to the next time step.

The time steps are chosen according to a few simple criteria. Since it is important that the weighted shape function integral, equation (77), remains constant over the interval this forms an obvious choice for time step selection. The time step criteria then is

$$\Delta t^{m+1} = \left| \int W(t^m) \frac{1}{v} S(t^m) - \int W(t^m) \frac{1}{v} S(t^{m+1}) \right| \div \xi_s \qquad 102$$

This then determines a maximum allowable time step. Other criteria have also been included to optimize the time step selection and are summarized below.

Time Step Selection

i) The following tests if true will set the maximum time step to one half of the previous time step.

   a) The maximum number of Δt^m iterations has been exceeded before equation (101) was satisfied.

   b) The criteria leading to the choice of time step in equation (102) has been exceeded such that

$$\left| \int W(t^m) \frac{1}{v} S(t^m) - \int W(t^m) \frac{1}{v} S(t^{m+1}) \right| > \xi_s \qquad 103$$

ii) An arbitrary maximum increase in time step of ten times the previous time step has been imposed.

iii) An average of the previous time steps is taken to smooth the increase in time steps such that

$$\Delta t^{m+1} = (1-\xi_a)\Delta t_*^{m+1} + \xi_a \bar{t}^m \qquad \text{i}$$

104

$$\bar{t}^{m+1} = (1-\xi_a)\Delta t^{m+1} + \xi_a \bar{t}^m \qquad \text{ii}$$

The * indicating the time step which would be chosen prior to the application of this equation.

The final resulting time step is chosen to be the smallest of the time steps indicated by the above criteria. Provision was also made for converging the time step at fixed intervals for the purpose of output.

Results and Discussion

The results in Appendix A are divided up into four cases each of which was chosen to accentuate a particular characteristic of the weighting schemes to be tested. The weighting schemes used will be referred to as Options 1 through 4 as defined below in our further discussions.

Option 1: Constant Steady State Adjoint weighting

Option 2: Constant value weighting

Option 3: Self weighting

Option 4: Adjusted thermal flux weighting

Option four is an additional variation of the self weighting scheme which uses an adjustment factor forcing the average point by point ratio of the fast component of the weighting function over the thermal component to be equal to that of the equivalent steady state adjoint ratio. This was accomplished using the relationship

105

$$W_f(r,E,t) = \frac{S_f(r,E,t) * S_{th}(r,E,t)}{S_f(r,E,t)} * AJW$$

where AJW is an input value. In practice AJW was adjusted to give approximately the same value for the integrated neutron lifetime at time zero as in the Option 1 case. Motivation for this variation came from the fact that the adjoint vector fast to thermal component ratio differs significantly from the flux vector fast to thermal component ratio, which is evident upon visual inspection of the adjoint shapes and flux shapes in the results, leading to a large difference in the reactivity and integrated neutron lifetime calculations. Also the

fast flux itself is usually very small in moderator regions and near external boundaries underestimating the neutron importance in these regions when used as a weighting function. The thermal flux was therefore considered to be a better approximation of the neutron importance in these regions. The need for a ratio adjustment is also supported by A.F. Henry[9] who states that the optimum weighting function is probably that function which optimizes calculational economy and has a fast to thermal ratio close in value to that of the adjoint function but need not be the adjoint function itself.

In each of the cases, which will be discussed individually below, the result of Option 1 will be considered the norm for comparison of the accuracy and efficiency of Options 2 to 4. Convergence criteria for each option will be identical to Option 1 whenever this is practical and will be redefined in the results where necessary.

Case 1: The purpose of this test case was to compare the performance of our program with an established benchmark case using the I.Q.S. method. The problem chosen came from the Argonne National Laboratory Benchmark Case Book[10] and is reproduced in the results. This case was run using the "QX1" code developed by D.A. Meneley, K.O. Ott and E.S. Wiener[11]. The weighting options tested include Options 1, 2 and 4. Option 3 was omitted from these recults due to the excessive cost involved in completing this run. This was the first indication of non ideal behaviour of Option 3 relative to the established Options 1 and 2.

Comparison of Option 1 results with the QX1 result indicates a significant difference in the amplitude value after four seconds transient. This can be attributed to the difference in the nodalization of the two programs, QX1 having cell edge nodes and our program having cell centered nodes. This is evident in the different k_{eff} values of the two programs at time zero and will lead to slightly different reactivity calculation results during the transient. Option 2 gave results which were slightly lower than Option 1 at four seconds but more significantly required more Δt^m time steps than Option 1 even with a reduced reactivity convergence

criteria value. From our development of the desirability of the adjoint weighting function this would be expected since this transient has a rather large change in flux shape. Option 4 gave results which were much higher than either of the Option 1 or 2 results. Increased convergence of the time steps showed no improvements in this result.

In spite of the differences between the results of Option 1 and the QX1 result, we can consider the code written to be suitable for the comparison of the different weighting schemes.

Case 2: Since the hypothesis on which our new weighting scheme, Option 3, was based is the near self adjointness of the Candu Heavy water moderated reactor an appropriate test of the weighting scheme is to compare its results with Options 1 and 2 in a self adjoint material system. The material system chosen for this test was artificially contrived using the material properties available in Case 1 as a basis. The transient chosen was not a very severe transient so that the results of all three options should be identical.

As expected the results of Options 1 and 2 were very close to each other, however, the result of Options 3 and 4 differed significantly from both of these. The number of shape function iterations and the cost of the four options were virtually identical as expected for a transient with a very small shape change.

Case 3: This case consists of a single material region reactor resulting in a very smooth flux shape. The purpose of this test is to demonstrate the feasibility of Option 3 or 4 in a non self adjoint material system with good near self adjoint shape characteristics. The appropriateness of a ratio adjustment in the weighting function will also be tested here.

Once again none of the Options 2 to 4 could match the result of Option 1. Option 2 required reduced convergence criteria to execute the problem within a reasonable number of time steps resulting in the difference between the Option 1 and 2 results. Similarly Option 3 also required reduced convergence criteria values. However, Option 4 did not require an adjustment of these criteria and needed

relatively few iterations to achieve a result. Even though this result does not compare well with Option 1, we do have an indication of the importance of the fast to thermal ratio in the point kinetics calculations.

Case 4: The purpose of this case was to demonstrate the effect of a large moderator region on the result of the self weighting scheme since this case was considered to show the least self adjointness. The material regions here are typical of a Candu type reactor and were obtained from course material.

In this case each of the options was run with the same convergence criteria with no significant difference in the number of shape function iterations. The Option 1 and 2 results are very close with the Options 3 and 4 being somewhat less than these.

Option 4 shows significant improvement over Option 3 with respect to Options 1 and 2 supporting the notion that the use of the fast neutron flux shape as a weighting function will lead to under-estimation of the reactivity in material systems with significantly large moderator regions.

Conclusions

The fact that our self weighting scheme has not performed as well as expected is most evident in the results of the test runs. However, we can make several important conclusions.

Firstly, we have demonstrated the importance of the fast to thermal flux ratio in the I.Q.S. time step calculations. It is shown that a ratio close in value to that of the adjoint function ratio lead to an improvement in the number of shape function calculation steps. This implies better self consistency of the result from one time step to the next. This effect was most pronounced in the Case 1, Option 3 runs which did not successfully run to four seconds within the limits of our computor account even with reduced convergence criteria while the Option 4 results showed no such difficulty. Improvements in the number of shape function calculation time steps appeared in Cases three and four also. The effect of this ratio on the amplitude function calculation however, was not significant as is demonstrated by the fact that the constant weighting scheme results were very close to the adjoint weighted results in all cases.

The second conclusion made is the fact that the thermal flux shape appears to be a better approximation to the adjoint flux shape than the fast neutron flux shape. In Case 4, Option 4 the result using the thermal flux shape is significantly closer to the adjoint weighted result than the Option 3 result. This supports the contention that the fast flux shape when used in the weighting scheme will underestimate the contribution to the reactivity in moderator regions of significant size.

Our third conclusion is based on the poor results of the Option 3 and 4 runs in each of the test cases. Since no mathematical or conceptual basis can be found for this discrepancy, we conclude

that some of the assumptions made in the implementation of this scheme are too crude. Increased convergence criteria showed no improvement of the results of the cases tested eliminating time dependence of the integrated neutron lifetime as a cause for concern. Further investigation into the cause of the discrepancy is warranted.

Appendix A:

Test Results: The following results are presented for each test case.

1) Neutron flux shape
2) Adjoint flux shape
3) Mean value of the ratios i: Fast adjoint over fast neutron flux
   ii: Thermal adjoint over thermal neutron flux
   iii: Fast adjoint over thermal adjoint

   along with the standard deviations(Std) of these point by point ratios.
4) Initial k_{eff}
5) Total power relative to the initial value and flux shape iteration step count versus time
6) Plotted thermal flux shape at time 0,1,2 and 4 seconds.
7) Regional power fractions at time 0,1,2 and 4 seconds.

The material region configuration used in all cases was as follows

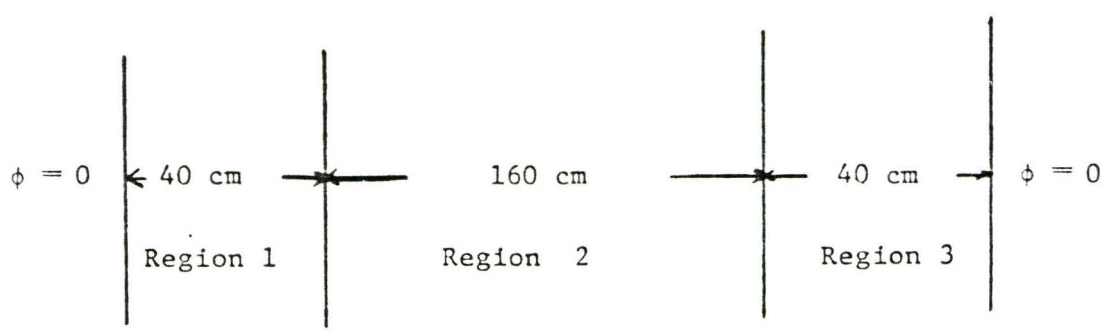

Figure 2

Test Case No. 1

Material Properties

Property		Initial Two Group Constants		
		Region 1	Region 2	Region 3
D^1	(cm)	1.50	1.00	1.50
D^2	(cm)	.50	.50	.50
Σ_a^1	(cm^{-1})	.026	.02	.026
Σ_a^2	(cm^{-1})	.18	.08	.18
$\nu\Sigma_f^1$	(cm^{-1})	.01	.005	.01
$\nu\Sigma_f^2$	(cm^{-1})	.20	.099	.20
Σ_s^{1-2}	(cm^{-1})	.015	.01	.015

Mesh spacing is 2 cm giving 120 mesh points.

Delayed Neutron Parameters

Type	Effective Delay Fraction	Decay Constant (sec^{-1})	
1	.00025	.0124	
2	.00164	.0305	
3	.00147	.1110	These parameters are
4	.00296	.3010	common to all test cases.
5	.00086	1.1400	
6	.00032	3.0100	

Initiating Perturbation: Σ_a^2 in region 1 is linearly decreased by 1% in 1 second.

Benchmark Comparsion run is the QX1 result

NEUTRON FLUX SHAPE: at time equals zero

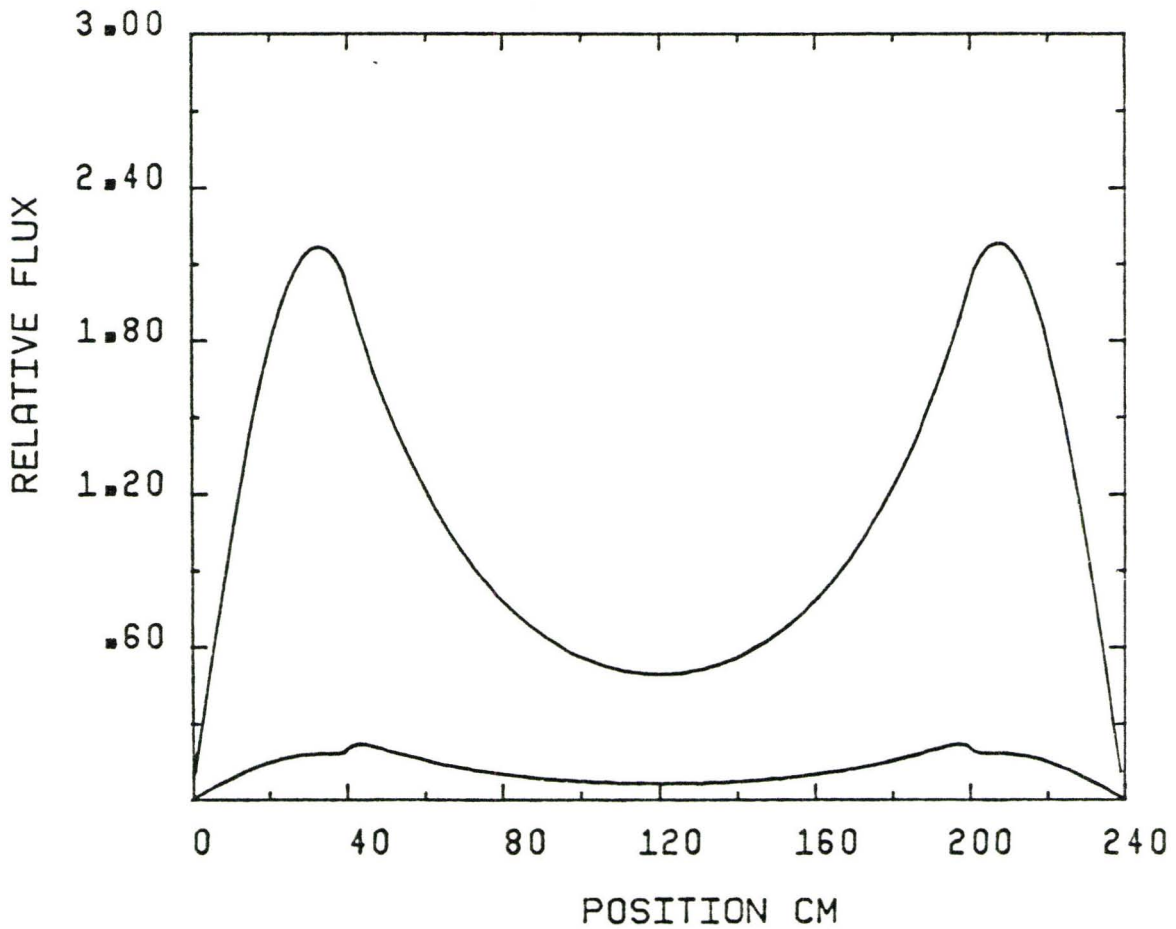

Figure 3

ADJOINT FLUX SHAPE: at time equals zero

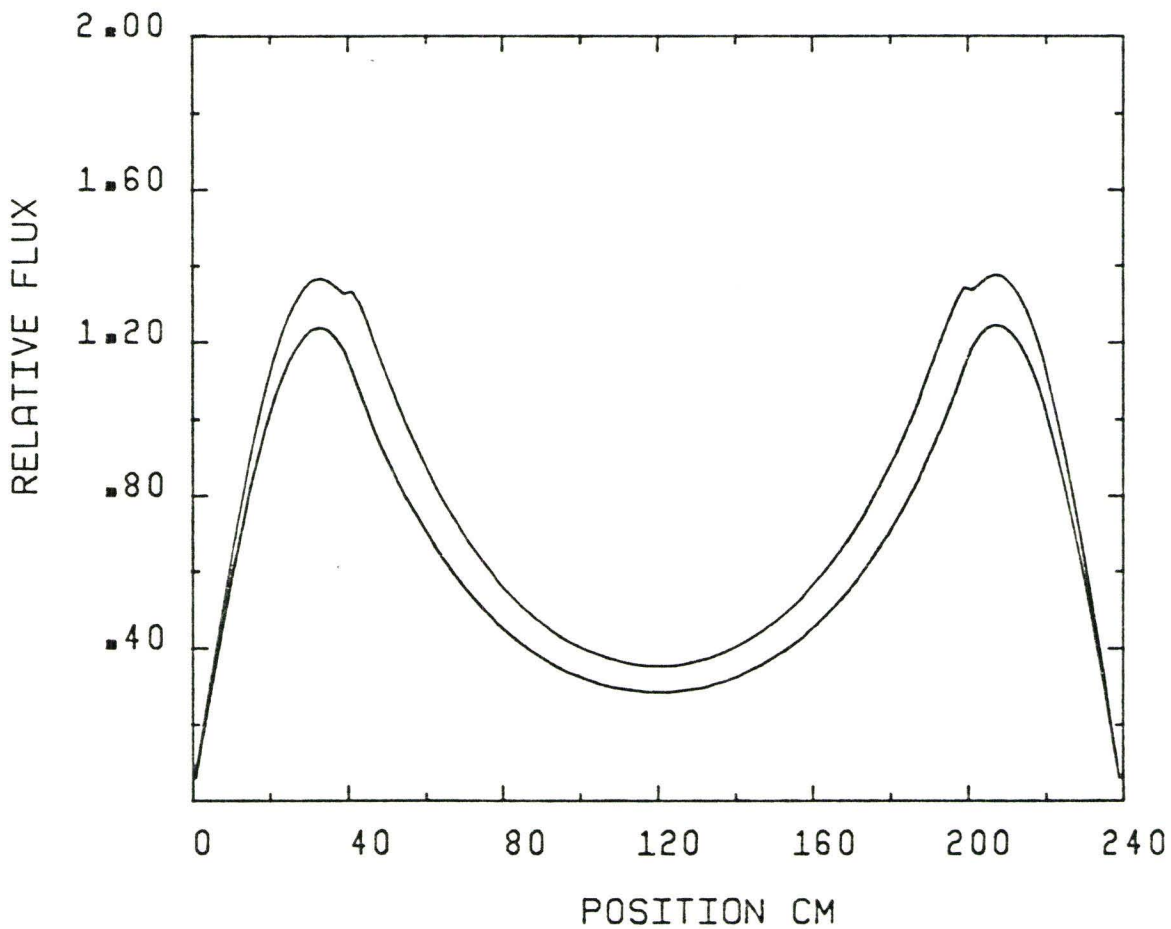

Ratios:	Mean	Std
i	.5754109	.0003682
ii	6.3540157	.0790873
iii	.8392259	.0042878

Figure 4

QX1 Results: ID.6-A2-3[10]

Initial k_{eff} 0.9015507

Initial power fractions

Region 1 0.27895
Region 2 0.44209
Region 3 0.27895

EXHIBIT A Total power (relative to initial value) and flux shape function count vs time.

EXHIBIT B Regional power (relative to initial value) vs time.

EXHIBIT A

Time (sec)	Total Power	Flux Shape Function No.[a]
0.0	1.000	1
0.1	1.028	5
0.2	1.063	7
0.5	1.205	12
1.0	1.740	26
1.5	1.959	33
2.0	2.166	37
3.0	2.606	43
4.0	3.108	48

[a]Cumulative up to the given time.

EXHIBIT B

	Relative Regional Power		
Time (sec)	Region 1	Region 2	Region 3
0.0	1.000	1.000	1.000
0.1	1.056	1.027	1.004
0.5	1.398	1.193	1.029
1.0	2.435	1.701	1.701
2.0	3.216	2.113	1.199
3.0	4.017	2.540	1.298
4.0	4.928	3.027	1.416

Option 1 Results

Convergence and Time Step Criteria

ξ_ϕ = .10 E-5
ξ_2 = .10 E-4 $\xi_1 = \xi_2$ 10.0 in all cases
ξ_s = .50 E-4
ξ_ρ = .50 E-4
ξ_a = .75

Initial k_{eff} = .901731

Relative Total Power

Time (sec)	Total Power	Flux Shape Step Iteration Number
0.0	1.000	1
0.1	1.028	10
0.2	1.063	12
0.5	1.204	21
1.0	1.727	37
1.5	1.940	47
2.0	2.145	51
3.0	2.571	58
4.0	3.059	64

Regional Power Fractions

Time (sec)	Region 1	Region 2	Region 3
0.0	.278067	.441967	.279966
1.0	.385937	.432106	.181956
2.0	.412096	.431291	.156613
3.0	.426951	.430832	.142216
4.0	.439738	.430449	.129813

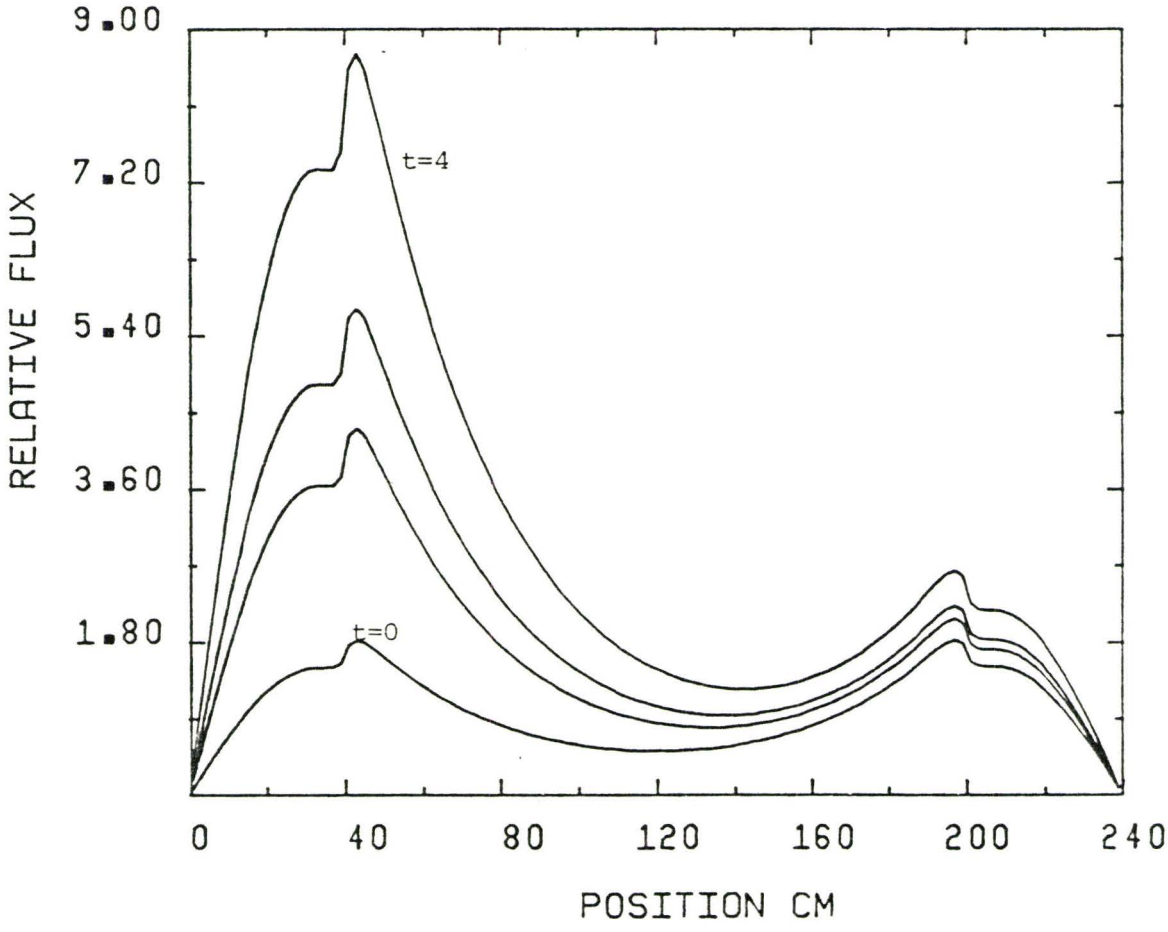
9.00
7.20
5.40
3.60
1.80
RELATIVE FLUX
t=4
t=0
0
40
80
120
160
200
240
POSITION CM

Figure 5

Option 2 Results

Convergence and Time Step Criteria: are the same as option 1 with the following exceptions

$\xi_s = .5\ E-2$

Relative Total Power

Time (sec)	Total Power	Flux Shape Step Iteration Number
0.0	1.000	1
0.1	1.028	20
0.2	1.061	22
0.5	1.200	27
1.0	1.718	46
1.5	1.926	54
2.0	2.126	58
3.0	2.541	65
4.0	3.030	72

Regional Power Fractions

Time (sec)	Region 1	Region 2	Region 3
0.0	.278067	.441967	.279966
1.0	.387989	.432037	.179975
2.0	.410562	.431336	.158103
3.0	.425505	.430875	.143620
4.0	.439048	.430468	.130484

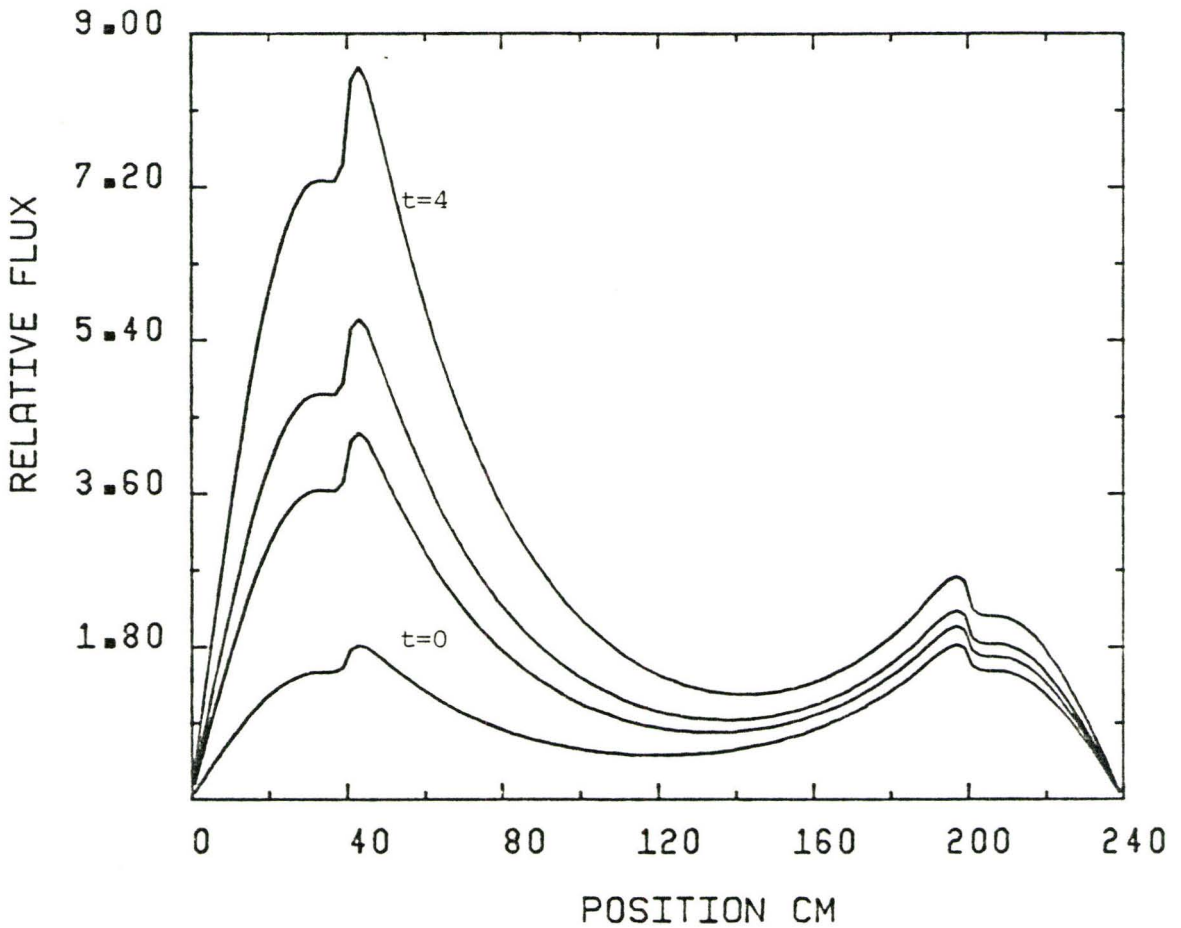
9.00
7.20
5.40
3.60
1.80
RELATIVE FLUX
t=4
t=0
0
40
80
120
160
200
240
POSITION CM

Figure 6

Option 4 Results

Convergence and Time Step Criteria: are the same as Option 1 with the following exceptions

$\xi_s = .5\ E\text{-}3$

Relative Total Power

Time (sec)	Total Power	Flux Shape Step Iteration Number
0.0	1.000	1
0.1	1.028	25
0.2	1.063	27
0.5	1.211	37
1.0	1.858	61
1.5	2.083	67
2.0	2.329	71
3.0	2.856	78
4.0	3.458	85

Regional Power Fractions

Time (sec)	Region 1	Region 2	Region 3
0.0	.278067	.441967	.279966
1.0	.386995	.432068	.180936
2.0	.412375	.431282	.156343
3.0	.427356	.430819	.141825
4.0	.440119	.430436	.129444

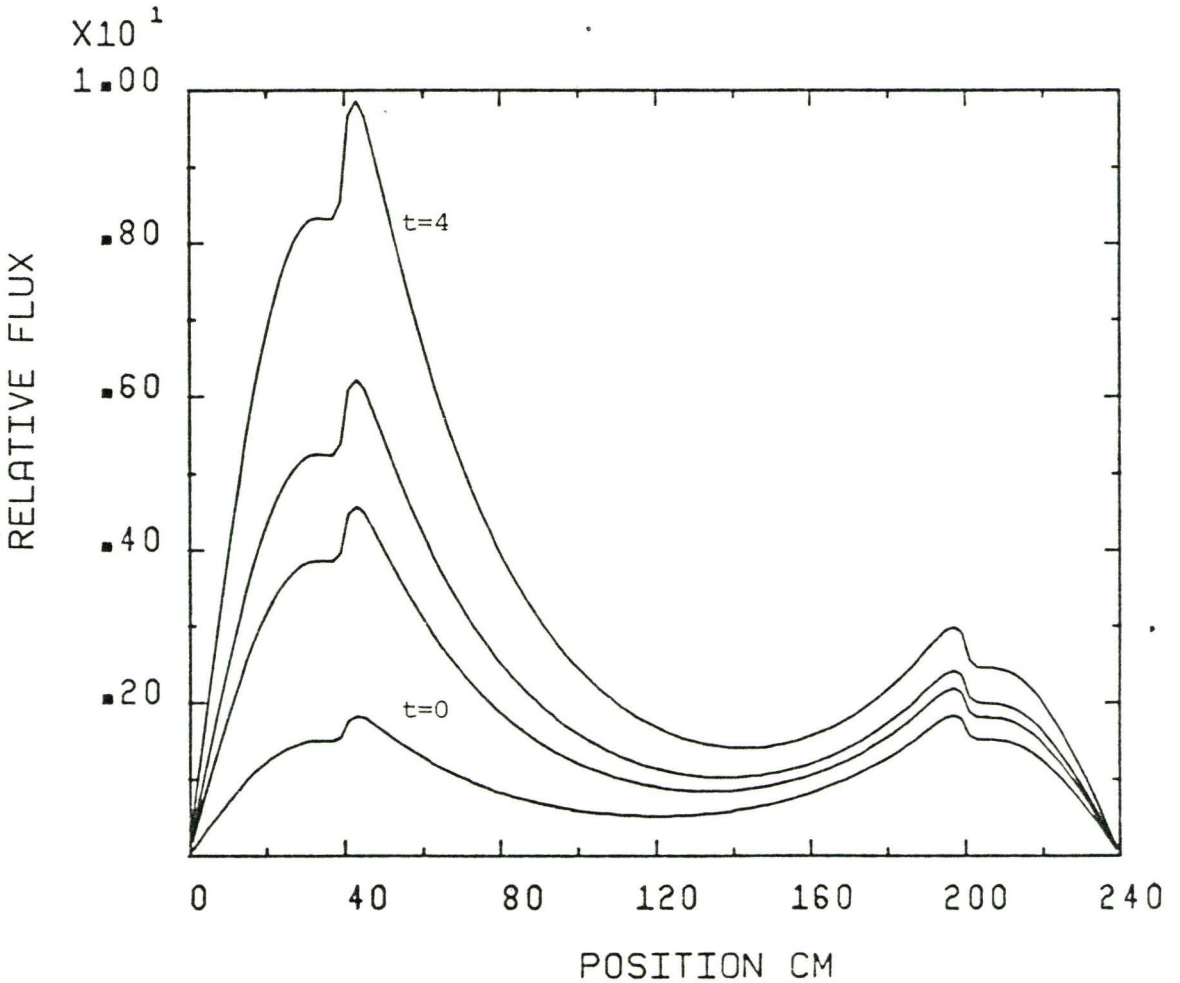
X10 1
1.00
.80
.60
.40
.20
RELATIVE FLUX
t=4
t=0
0
40
80
120
160
200
240
POSITION CM

Figure 7

Test Case No. 2

Material Properties: The material properties of all three regions are the same as that of region 1 in test case no. 1 with the following exceptions.

$\nu\Sigma_f^2$ (cm^{-1}) = .05525

$\Sigma^{1-2}(cm^{-1})$ = .05525

Mesh spacing is 8 cm giving 30 mesh points

Initiating Perturbation: Σ_a^2 in region 1 is linearly decreased by 5.0% in 1 second

No benchmark comparison run

NEUTRON and ADJOINT FLUX SHAPE: at time equals zero

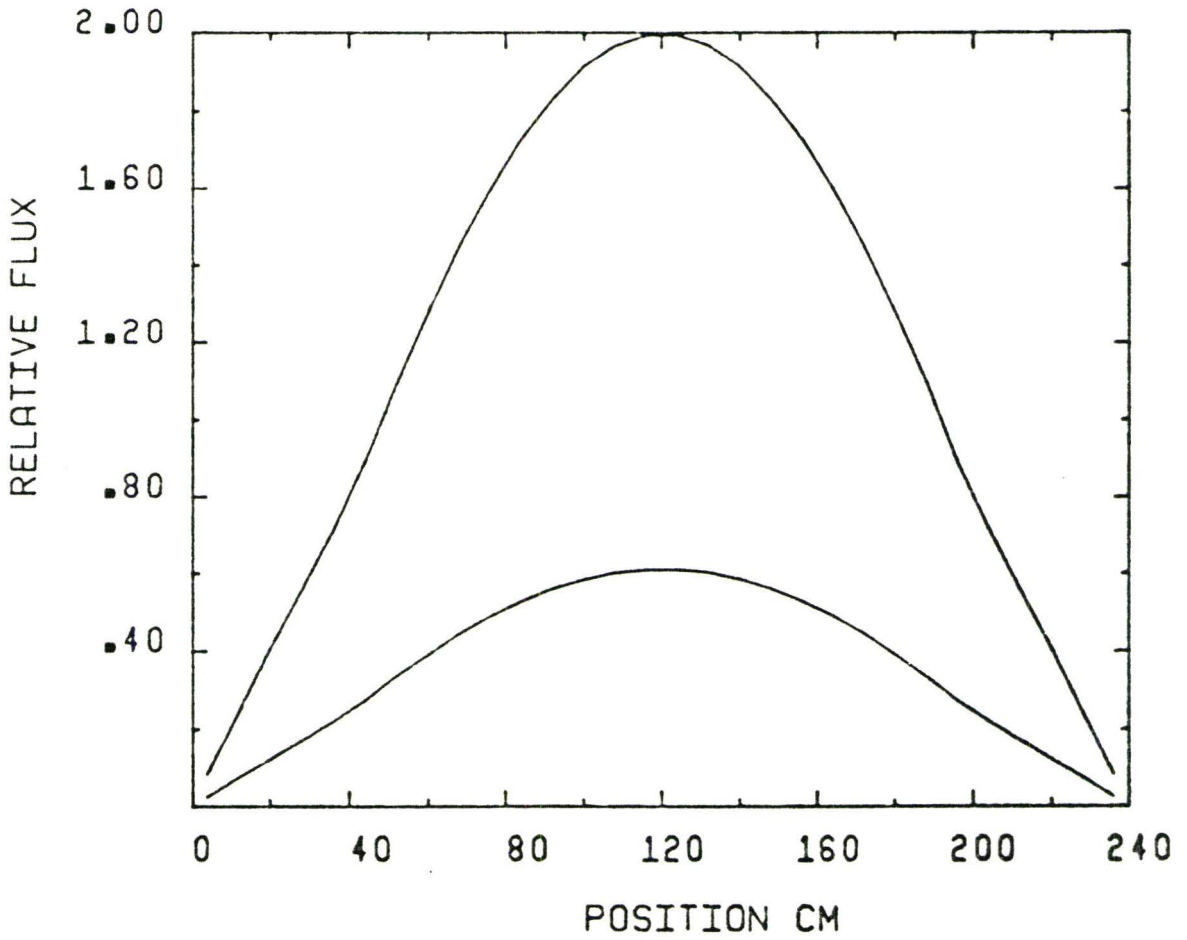

Ratios:	Mean	Std
i and ii	Not applicable	
iii	.8392259	.0042878

Figure 8

Option 1 Results

Convergence and Time Step Criteria

ξ_{ϕ} = .10 E-5
ξ_{2} = .10 E-4
ξ_{s} = .10 E-3
ξ_{ρ} = .25 E-4
ξ_{a} = .75

Initial k_{eff} = 1.02809

Relative Total Power

Time (sec)	Total Power	Flux Shape Step Iteration Number
0.0	1.000	1
0.1	1.009	8
0.2	1.018	9
0.5	1.054	16
1.0	1.149	28
1.5	1.170	37
2.0	1.188	41
3.0	1.220	49
4.0	1.250	57

Regional Power Fractions

Time (sec)	Region 1	Region 2	Region 3
0.0	.056434	.887146	.056420
1.0	.077755	.869945	.052300
2.0	.078327	.869599	.052075
3.0	.078683	.869389	.051928
4.0	.079017	.869189	.051795

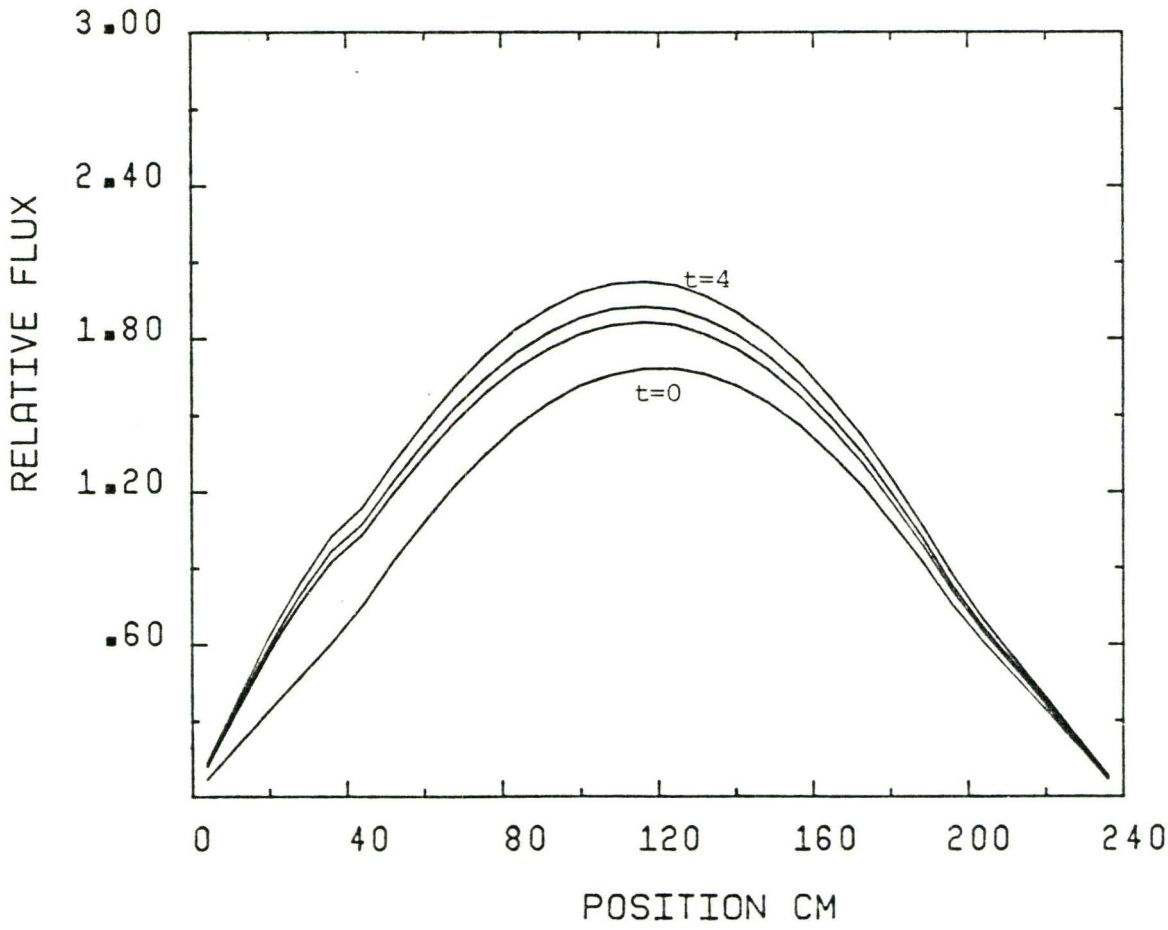
3.00
2.40
1.80
1.20
.60
RELATIVE FLUX
t=4
t=0
0
40
80
120
160
200
240
POSITION CM

Figure 9

Option 2 Results

Convergence and Time Step Criteria: Same as option 1

Relative Total Power

Time (sec)	Total Power	Flux Shape Step Iteration Number
0.0	1.000	1
0.1	1.009	8
0.2	1.018	9
0.5	1.054	16
1.0	1.149	28
1.5	1.170	37
2.0	1.188	41
3.0	1.220	49
4.0	1.250	57

Regional Power Fractions

Time (sec)	Region 1	Region 2	Region 3
0.0	.056434	.887146	.056420
1.0	.077755	.869945	.052300
2.0	.078327	.869599	.052075
3.0	.078730	.869358	.051912
4.0	.078979	.869215	.051807

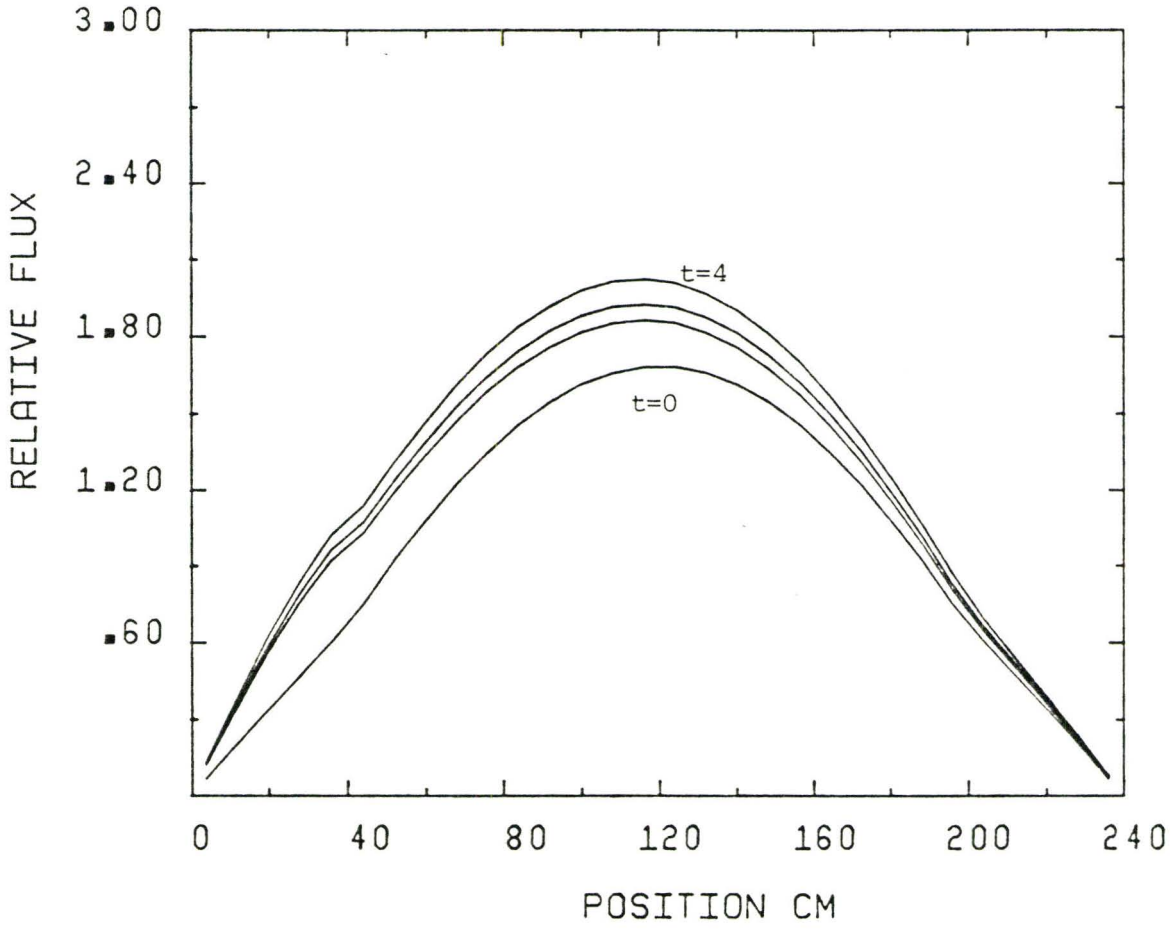
3.00
2.40
1.80
1.20
.60
RELATIVE FLUX
t=4
t=0
0
40
80
120
160
200
240
POSITION CM

Figure 10

Option 3 Results

Convergence and Time Step Criteria: same as option 1

Relative Total Power

Time (sec)	Total Power	Flux Shape Step Iteration Number
0.0	1.000	1
0.1	1.008	9
0.2	1.018	10
0.5	1.054	16
1.0	1.152	28
1.5	1.174	37
2.0	1.192	41
3.0	1.224	49
4.0	1.254	57

Regional Power Fractions

Time (sec)	Region 1	Region 2	Region 3
0.0	.056434	.887146	.056420
1.0	.077672	.870006	.052322
2.0	.078325	.869599	.052075
3.0	.078729	.869358	.051913
4.0	.079015	.869189	.051795

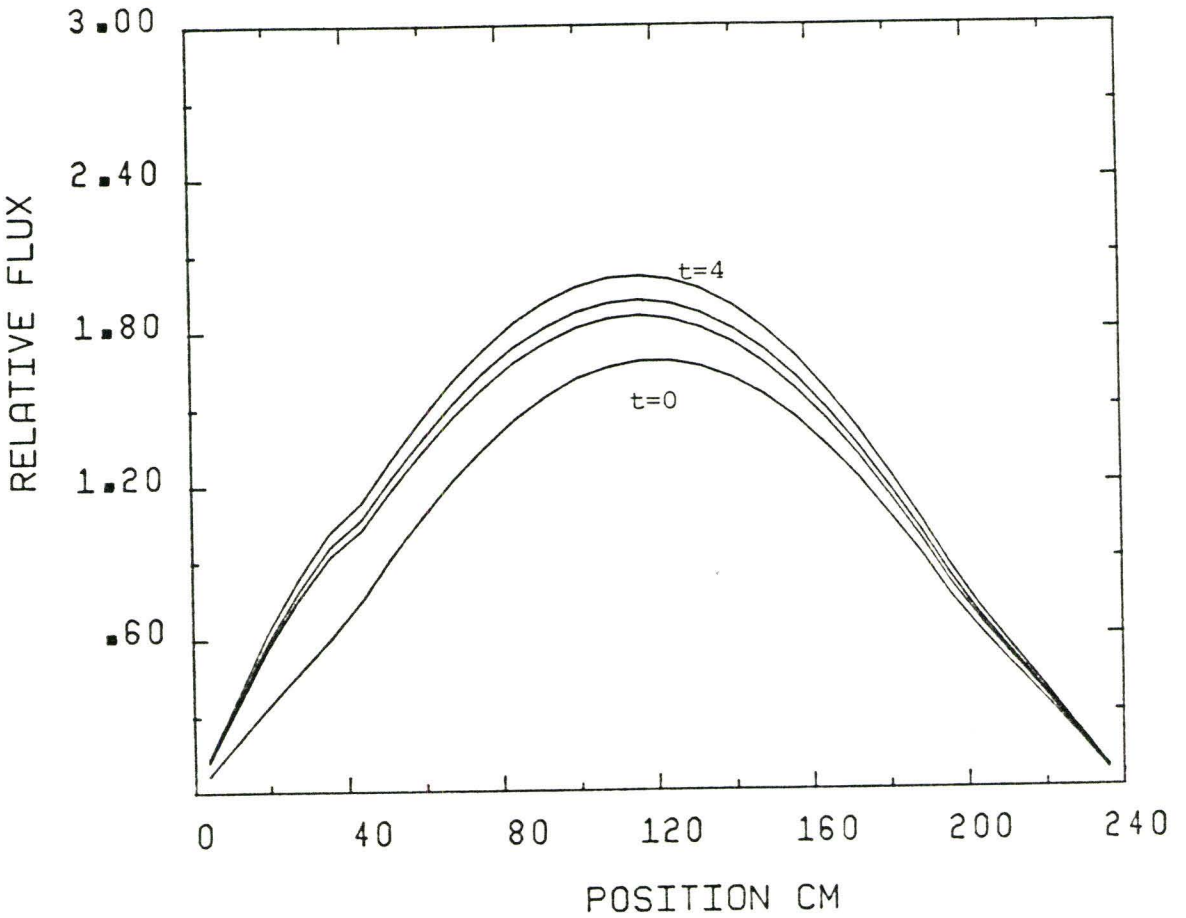
3.00
2.40
1.80
1.20
.60
RELATIVE FLUX
t=4
t=0
0
40
80
120
160
200
240
POSITION CM

Figure 11

Option 4 Results

Convergence and Time Step Criteria: same as option 1

Relative Total Power

Time (sec)	Total Power	Flux Shape Step Iteration Number
0.0	1.000	1
0.1	1.008	9
0.2	1.018	10
0.5	1.054	16
1.0	1.152	28
1.5	1.174	36
2.0	1.192	40
3.0	1.224	48
4.0	1.254	56

Regional Power Fractions

Time (sec)	Region 1	Region 2	Region 3
0.0	.056434	.887146	.056420
1.0	.077750	.869948	.052302
2.0	.078326	.869599	.052075
3.0	.078729	.869358	.051913
4.0	.079014	.869190	.051796

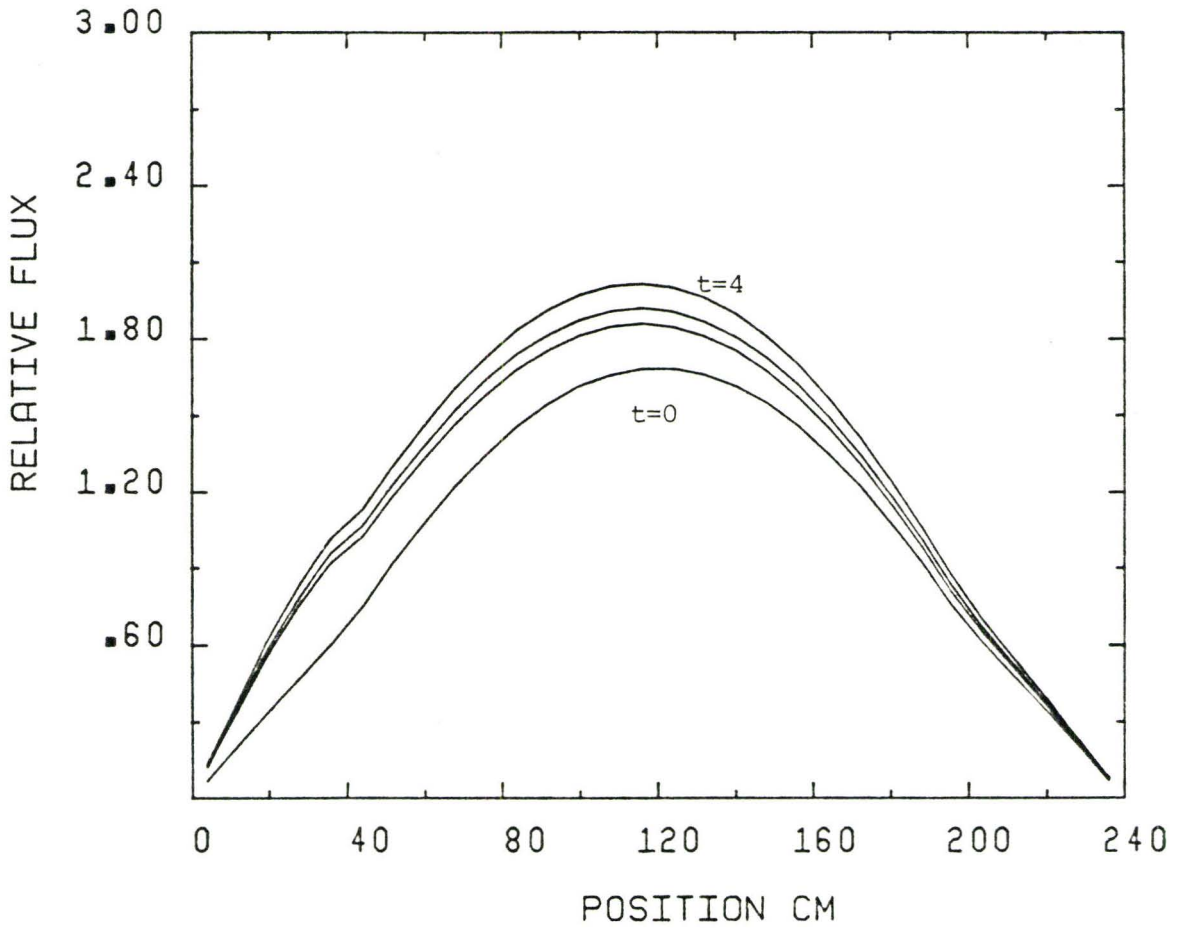
3.00
2.40
1.80
1.20
.60
RELATIVE FLUX
t=4
t=0
0
40
80
120
160
200
240
POSITION CM

Figure 12

Test Case No. 3

Material Properties: The material properties of all three regions are the same as region 2 of test case no. 1 with the following exceptions.

$D^1 = 1.50$

Mesh spacing is 8 cm giving 30 mesh points

Initiating Perturbation: a^2 in region 1 is linearly decreased by 5% in 1 second

No benchmark comparison run

NEUTRON FLUX SHAPE

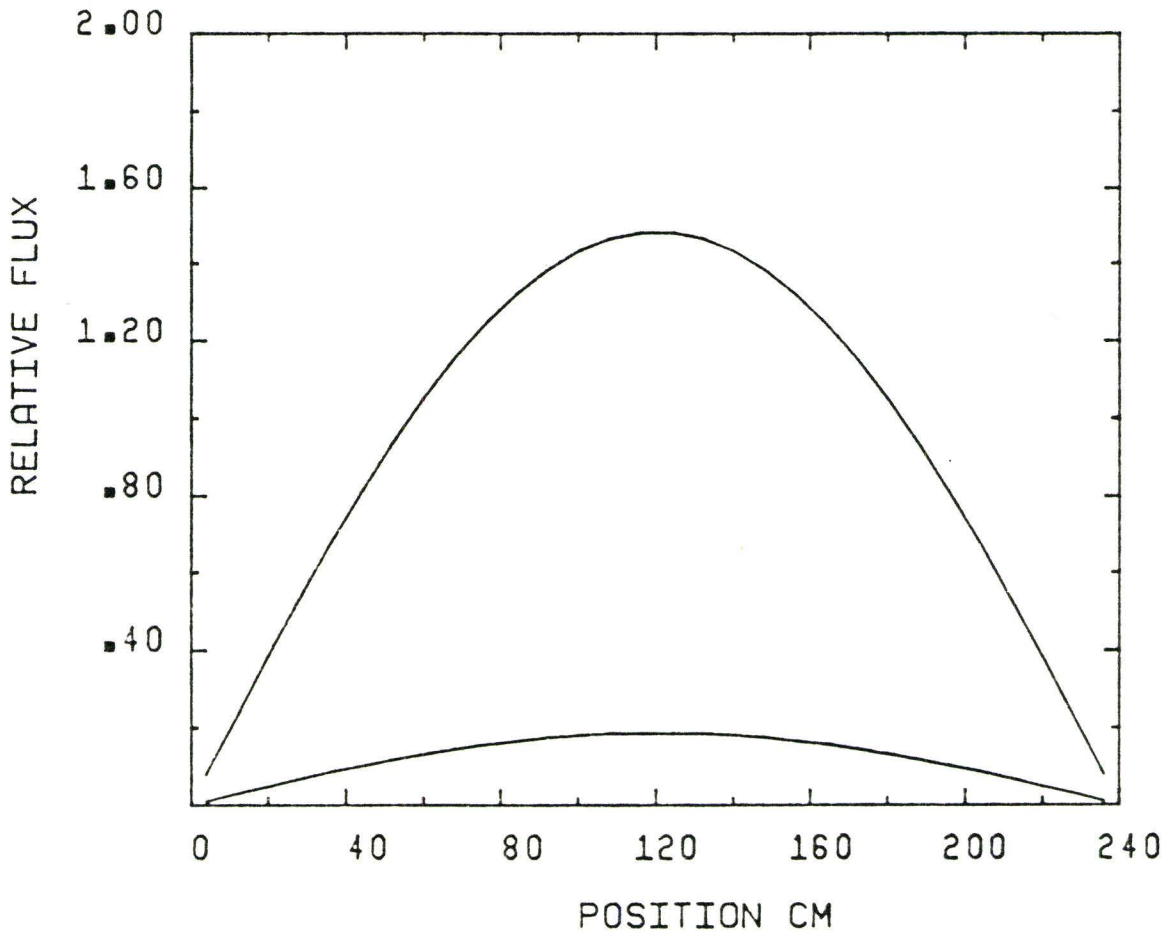

Figure 13

ADJOINT FLUX SHAPE

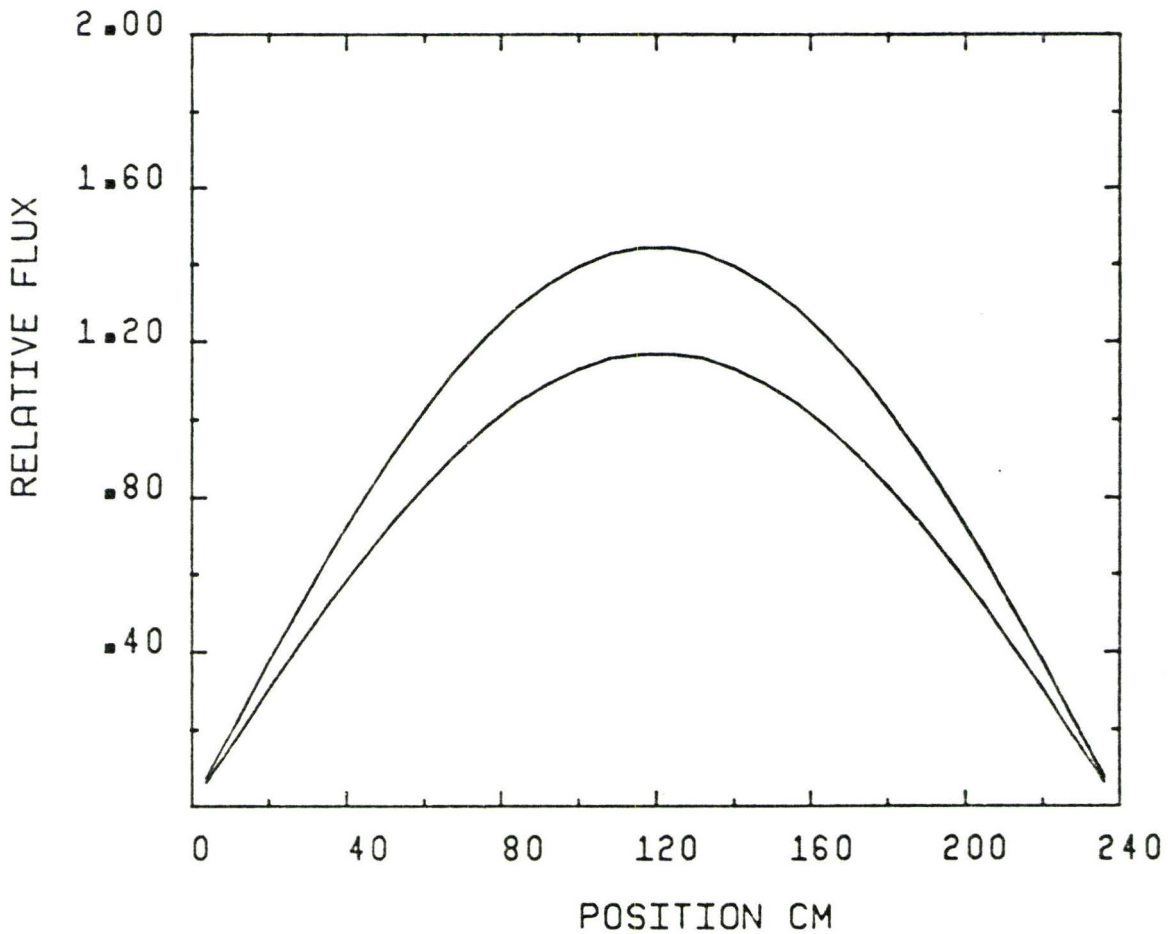

Ratios	Mean	Std
i	.7878652	.0000438
ii	7.8001423	.0002741
iii	.8089540	.0000209

Figure 14

Option 1 Results

Convergence and Time Step Criteria

ξ_{ϕ} = .10 E-5

ξ_2 = .10 E-4

ξ_s = .10 E-3

ξ_{ρ} = .25 E-4

ξ_a = .75

Initial k_{eff} = .857084

Relative Total Power

Time (sec)	Total Power	Flux Shape Step Iteration Number
0.0	1.000	1
0.1	1.013	7
0.2	1.030	10
0.5	1.089	19
1.0	1.249	37
1.5	1.289	46
2.0	1.321	50
3.0	1.381	58
4.0	1.436	66

Regional Power Fractions

Time (sec)	Region 1	Region 2	Region 3
0.0	.066994	.866025	.066981
1.0	.086122	.851541	.062337
2.0	.086480	.851358	.062162
3.0	.086709	.851243	.062049
4.0	.086867	.851164	.061970

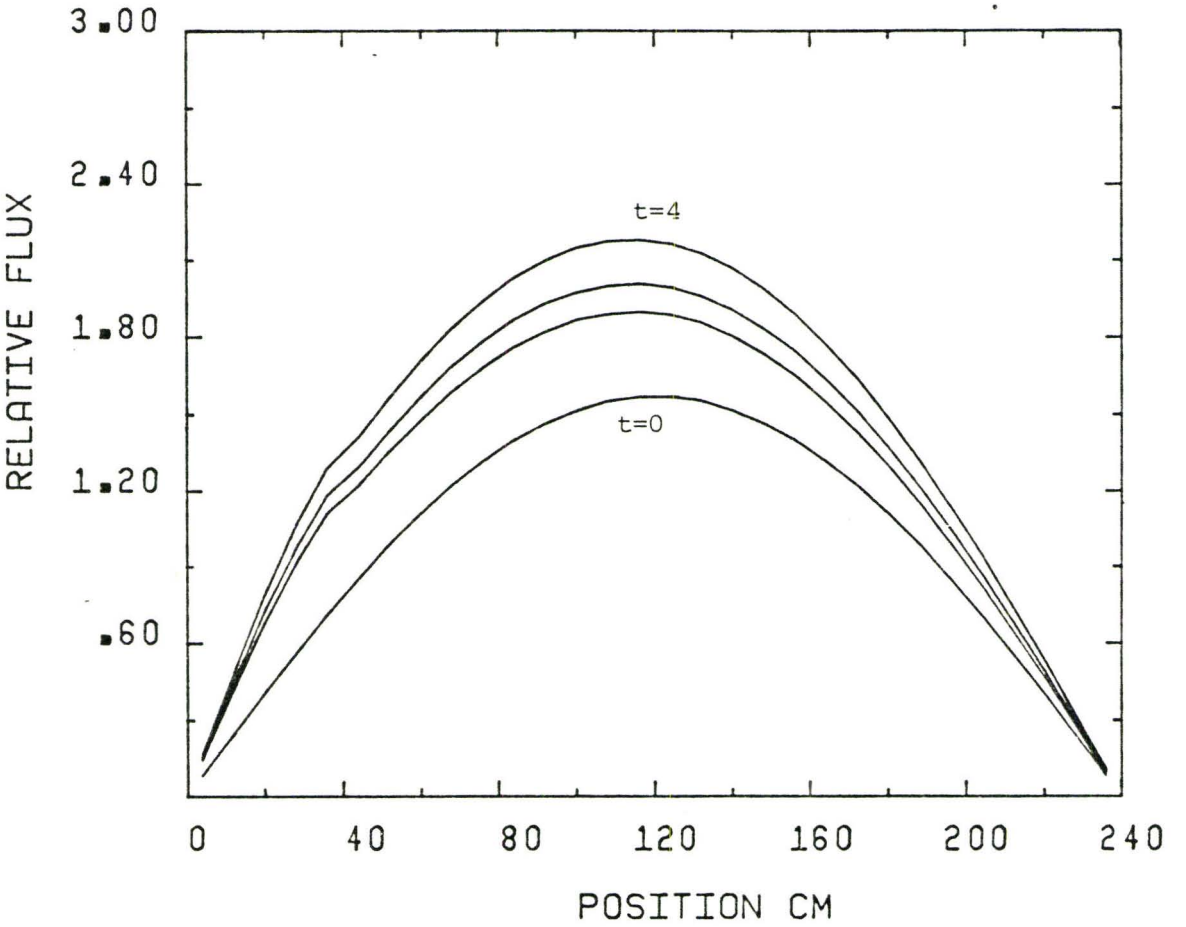
3.00
2.40
1.80
1.20
.60
RELATIVE FLUX
t=4
t=0
0
40
80
120
160
200
240
POSITION CM

Figure 15

Option 2 Results

Convergence and Time Step Criteria: Same as option 1 with the following exception

$\xi_s = .75\ E\text{-}3$

Relative Total Power

Time (sec)	Total Power	Flux Shape Step Iteration Number
0.0	1.000	1
0.1	1.015	31
0.2	1.032	33
0.5	1.096	46
1.0	1.266	62
1.5	1.307	72
2.0	1.340	76
3.0	1.400	84
4.0	1.457	92

Regional Power Fractions

Time (sec)	Region 1	Region 2	Region 3
0.0	.066994	.866025	.066981
1.0	.086140	.851532	.062328
2.0	.086481	.851358	.062162
3.0	.086709	.851242	.062049
4.0	.086865	.851164	.061971

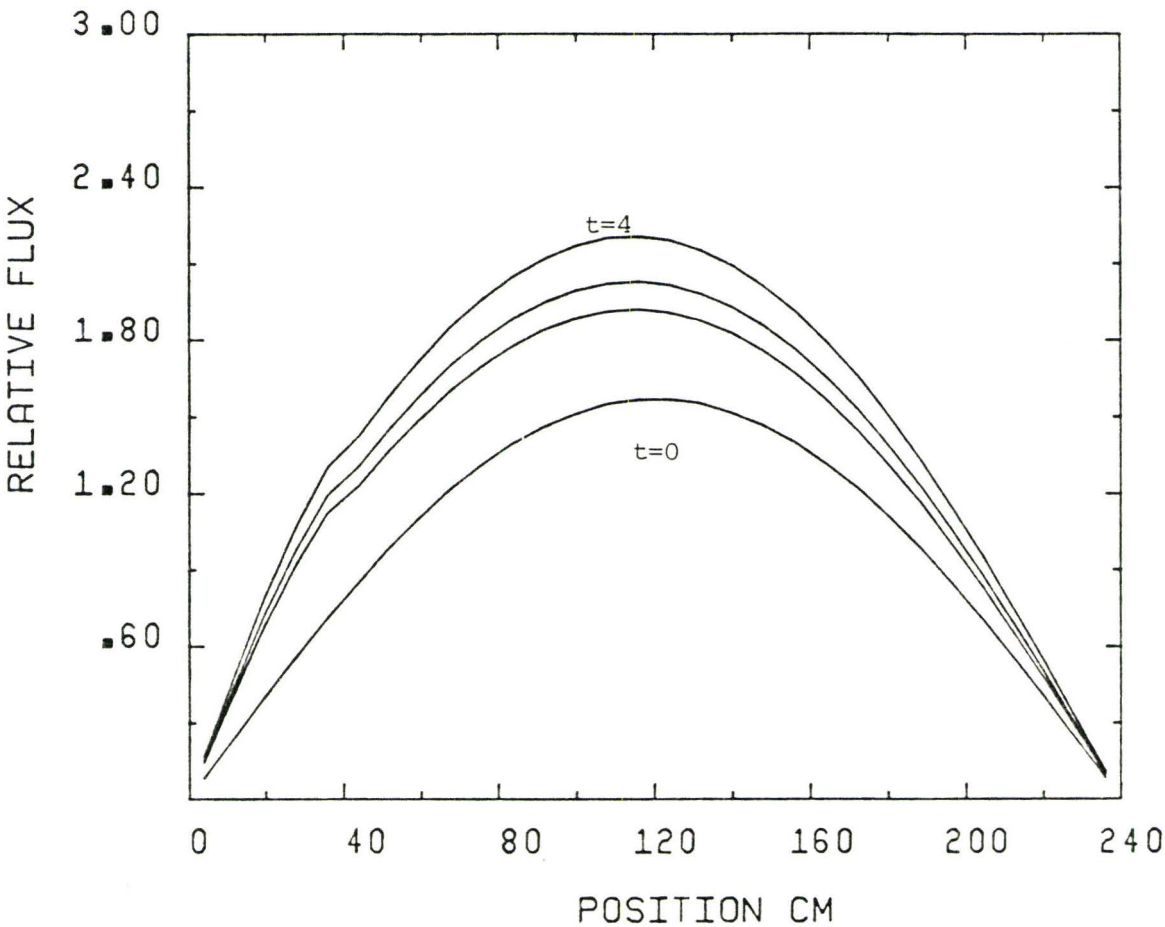
3.00
2.40
1.80
1.20
.60
RELATIVE FLUX
t=4
t=0
0
40
80
120
160
200
240
POSITION CM

Figure 16

Option 3 Results

Convergence and Time Step Criteria: Same as option 1 with the following exceptions

ξ_c = .75 E-3

Relative Total Power

Time (sec)	Total Power	Flux Shape Step Iteration Number
0.0	1.000	1
0.1	1.014	22
0.2	1.030	24
0.5	1.090	35
1.0	1.252	56
1.5	1.291	64
2.0	1.324	68
3.0	1.383	76
4.0	1.439	84

Regional Power Fractions

Time (sec)	Region 1	Region 2	Region 3
0.0	.066994	.866025	.066981
1.0	.086144	.851530	.062326
2.0	.086477	.851359	.062164
3.0	.086706	.851243	.062051
4.0	.086864	.851164	.061972

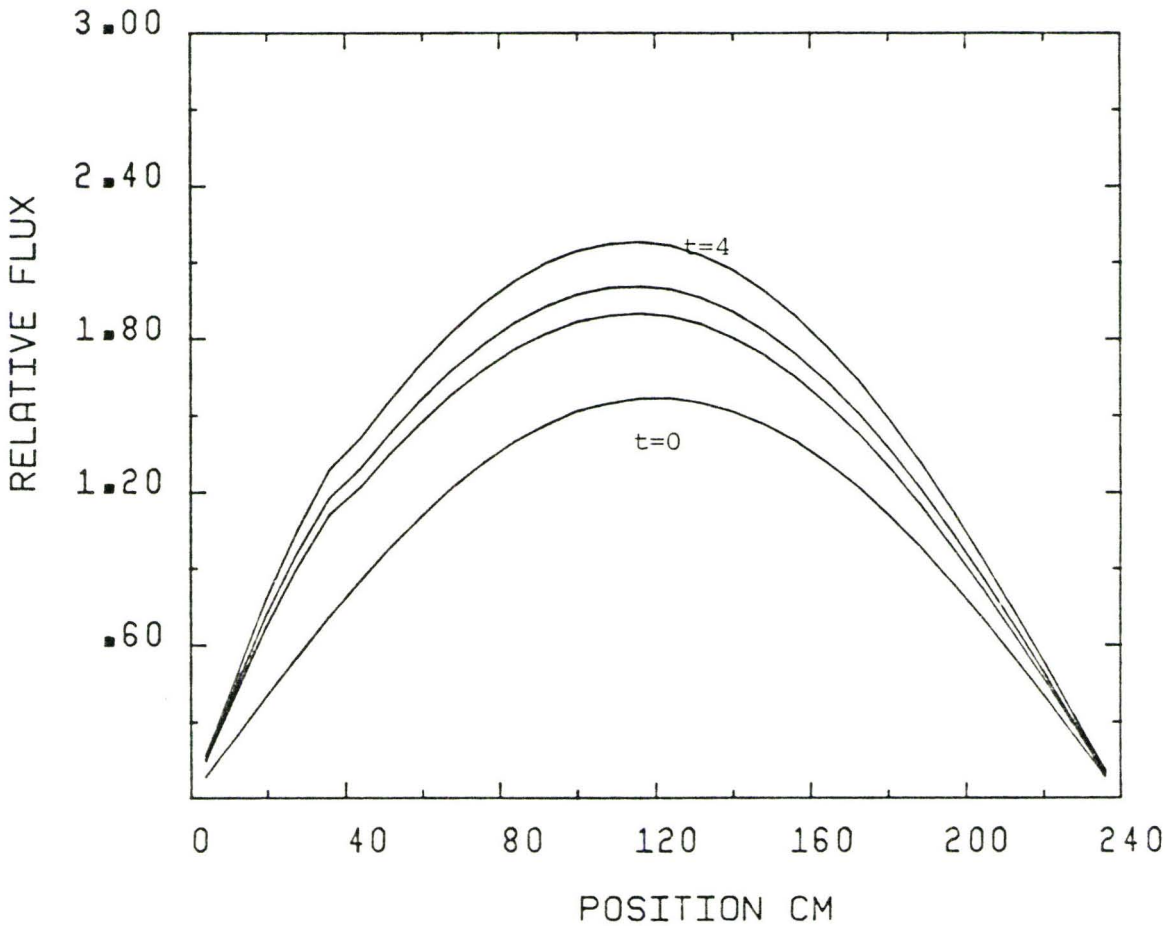
3.00
2.40
1.80
1.20
.60
RELATIVE FLUX
t=4
t=0
0
40
80
120
160
200
240
POSITION CM

Figure 17

Option 4 Results

Convergence and Time Step Criteria: Same as option 1

Relative Total Power

Time (sec)	Total Power	Flux Shape Step Iteration Number
0.0	1.000	1
0.1	1.015	7
0.2	1.030	10
0.5	1.090	17
1.0	1.252	35
1.5	1.292	44
2.0	1.325	48
3.0	1.384	56
4.0	1.440	64

Regional Power Fractions

Time (sec)	Region 1	Region 2	Region 3
0.0	.066994	.866025	.066981
1.0	.086144	.851530	.062326
2.0	.086478	.851359	.062164
3.0	.086706	.851243	.062050
4.0	.086864	.851164	.061972

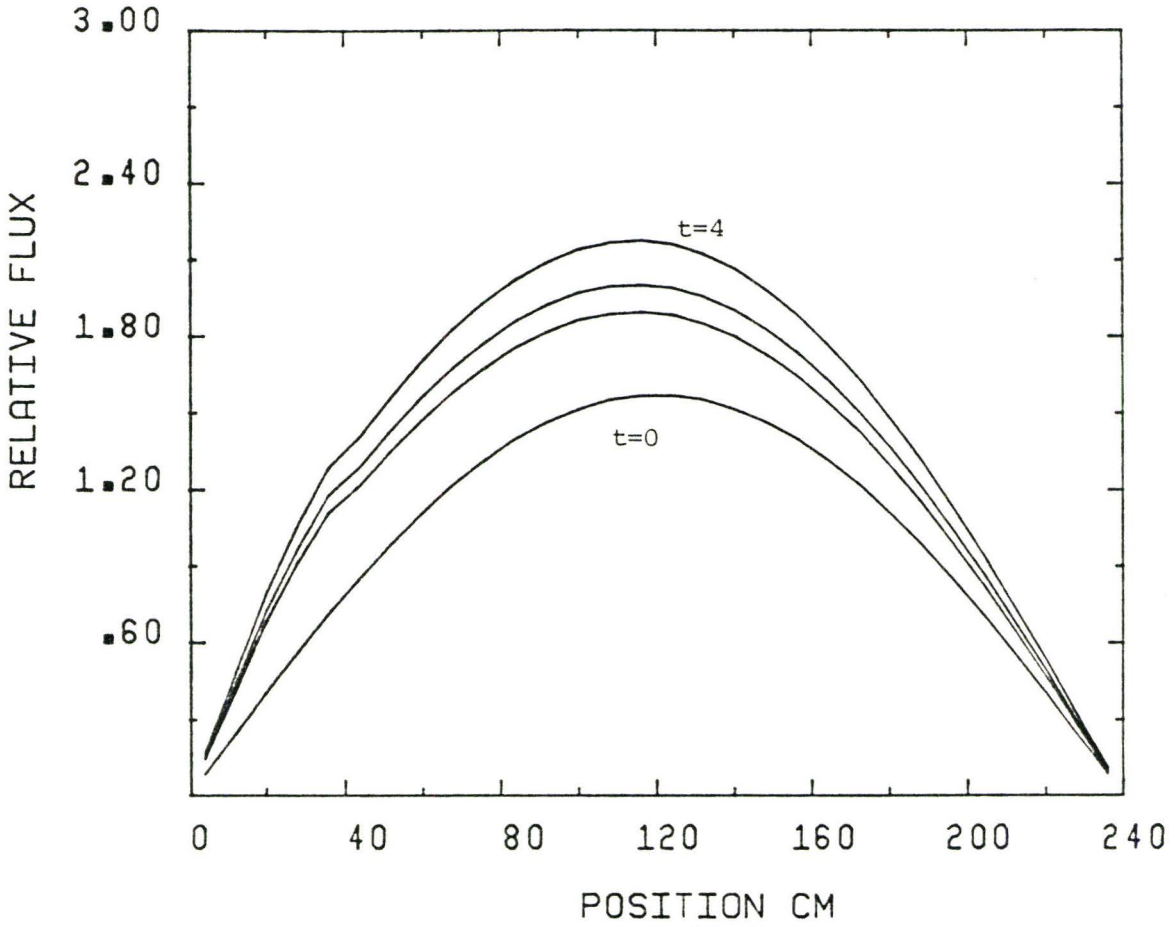
3.00
2.40
1.80
1.20
.60
RELATIVE FLUX
t=4
t=0
0
40
80
120
160
200
240
POSITION CM

Figure 18

Test Case No. 4

Material Properties

Property		Initial Two Group Constants		
		Region 1	Region 2	Region 3
D^1	(cm)	1.2651	1.2651	1.2651
D^2	(cm)	.9329	.9329	.9329
Σ_a^1	(cm^{-1})	1.0197E-2	8.56434E-3	1.0197E-3
Σ_a^2	(cm^{-1})	8.5487E-5	4.0423 E-3	8.5487E-5
$\nu\Sigma_f^1$	(cm^{-1})	0.0	0.0	0.0
$\nu\Sigma_f^2$	(cm^{-1})	0.0	4.8517 E-3	0.0
Σ_s^{1-2}		1.0197E-2	7.6835 E-3	1.0197E-2

Mesh spacing is 8 cm giving 30 mesh points

Delayed Neutron parameters are the same as case no. 1.

Initiating Perturbation: Σ_a^2 in region 2 is linearly decreased by .25% in 1 second

No benchmark comparision case.

NEUTRON FLUX SHAPE:at time equals zero

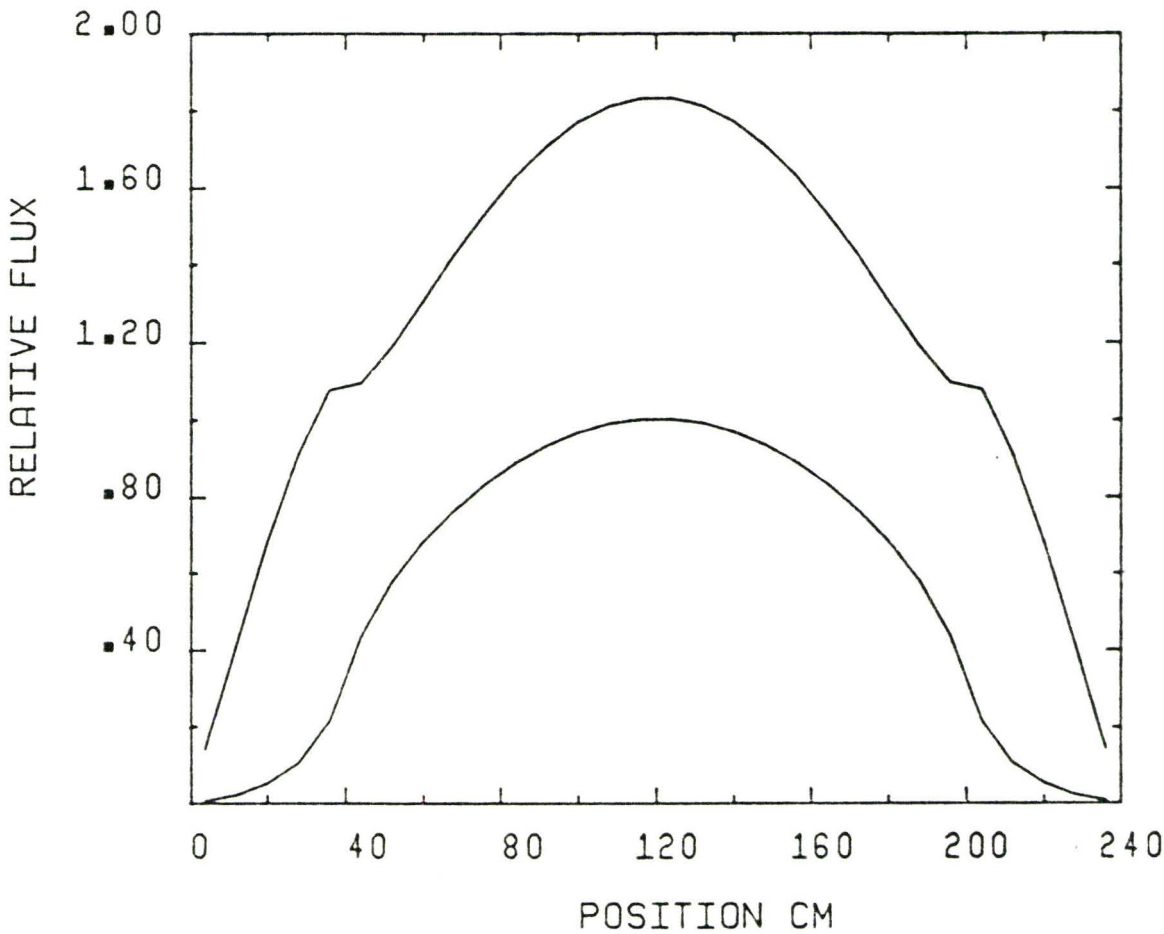

Figure 19

ADJOINT FLUX SHAPE

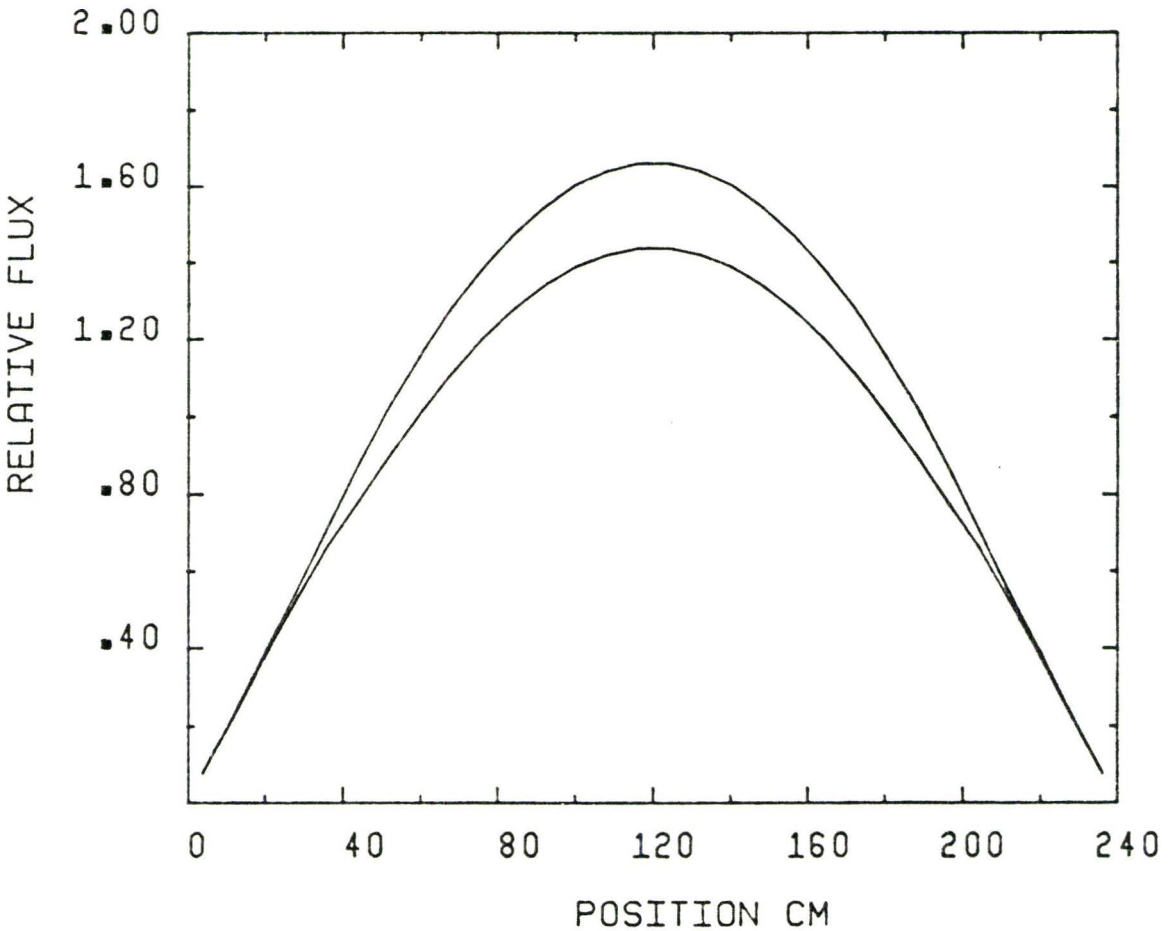

Ratios:	Including Moderator Region		Excluding Moderator region	
	Mean	Std	Mean	Std
i	3.456588	.4640520	1.487912	.0249958
ii	.787123	.0247569	.887315	.0075371
iii	.902715	.0076858	.870872	.0017020

Figure 20

Option 1 Results

Convergence and Time Step Criteria

ξ_{ϕ} = .10 E-5
ξ_{2} = .10 E-4
ξ_{ρ} = .10 E-3
ξ_{s} = .25 E-4
ξ_{a} = .75

Initial k_{eff} = 1.00856

Relative Total Power

Time (sec)	Total Power	Flux Shape Step Iteration Number
0.0	1.000	1
0.1	1.010	10
0.2	1.035	14
0.5	1.143	32
1.0	1.421	61
1.5	1.500	77
2.0	1.694	82
3.0	1.866	90
4.0	2.034	98

Regional Power Fractions

Time (sec)	Region 1	Region 2	Region 3
0.0	0.0	1.0	0.0
1.0	0.0	1.0	0.0
2.0	0.0	1.0	0.0
3.0	0.0	1.0	0.0
4.0	0.0	1.0	0.0

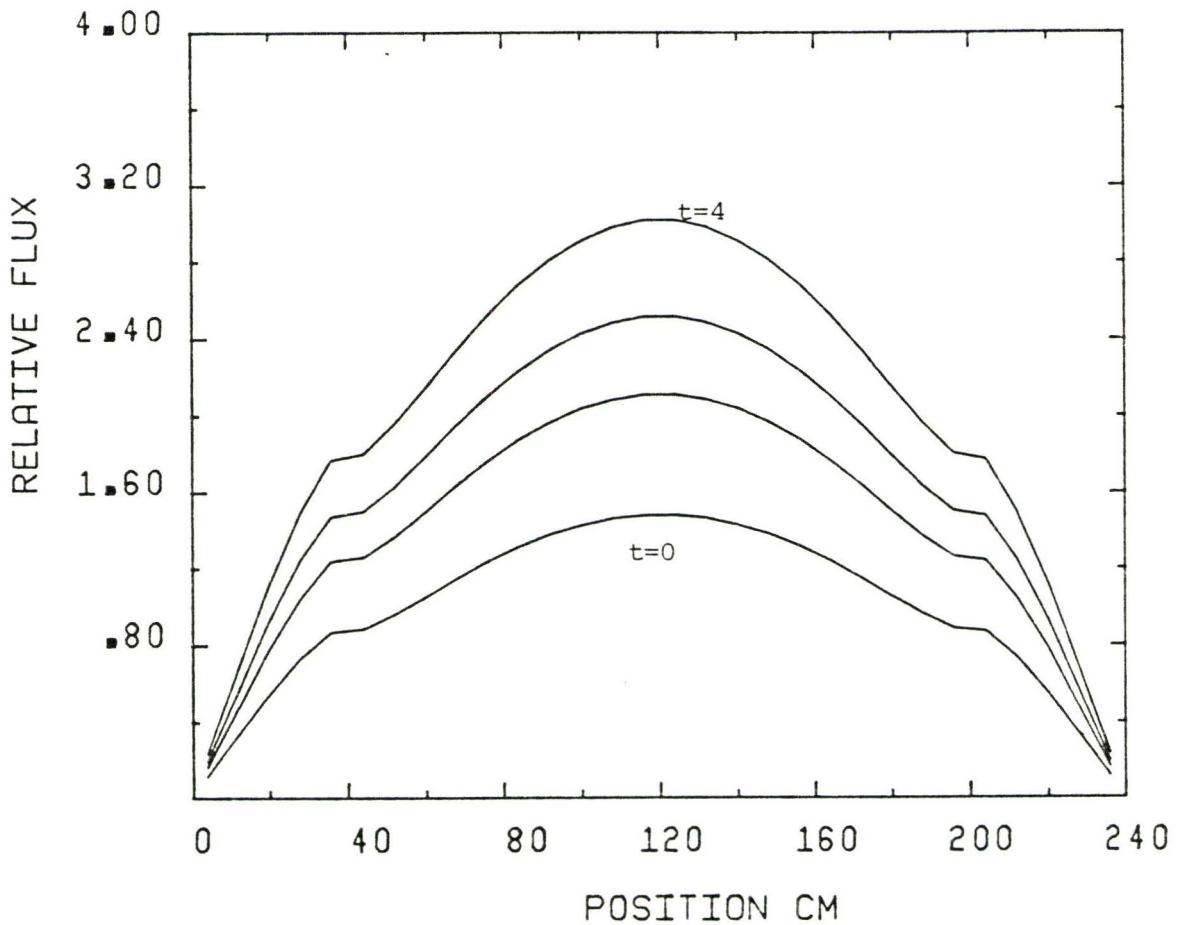
4.00
3.20
2.40
1.60
.80
RELATIVE FLUX
t=4
t=0
0
40
80
120
160
200
240
POSITION CM

Figure 21

Option 2 Results

Convergence and Time Step Criteria: same as option 1

Relative Total Power

Time (sec)	Total Power	Flux Shape Step Iteration Number
0.0	1.000	1
0.1	1.010	13
0.2	1.035	17
0.5	1.143	34
1.0	1.423	62
2.0	1.600	73
3.0	1.867	87
4.0	2.035	95

Regional Power Fractions: Region 1 and 2 power fractions are zero with region 2 power fractions equal to one.

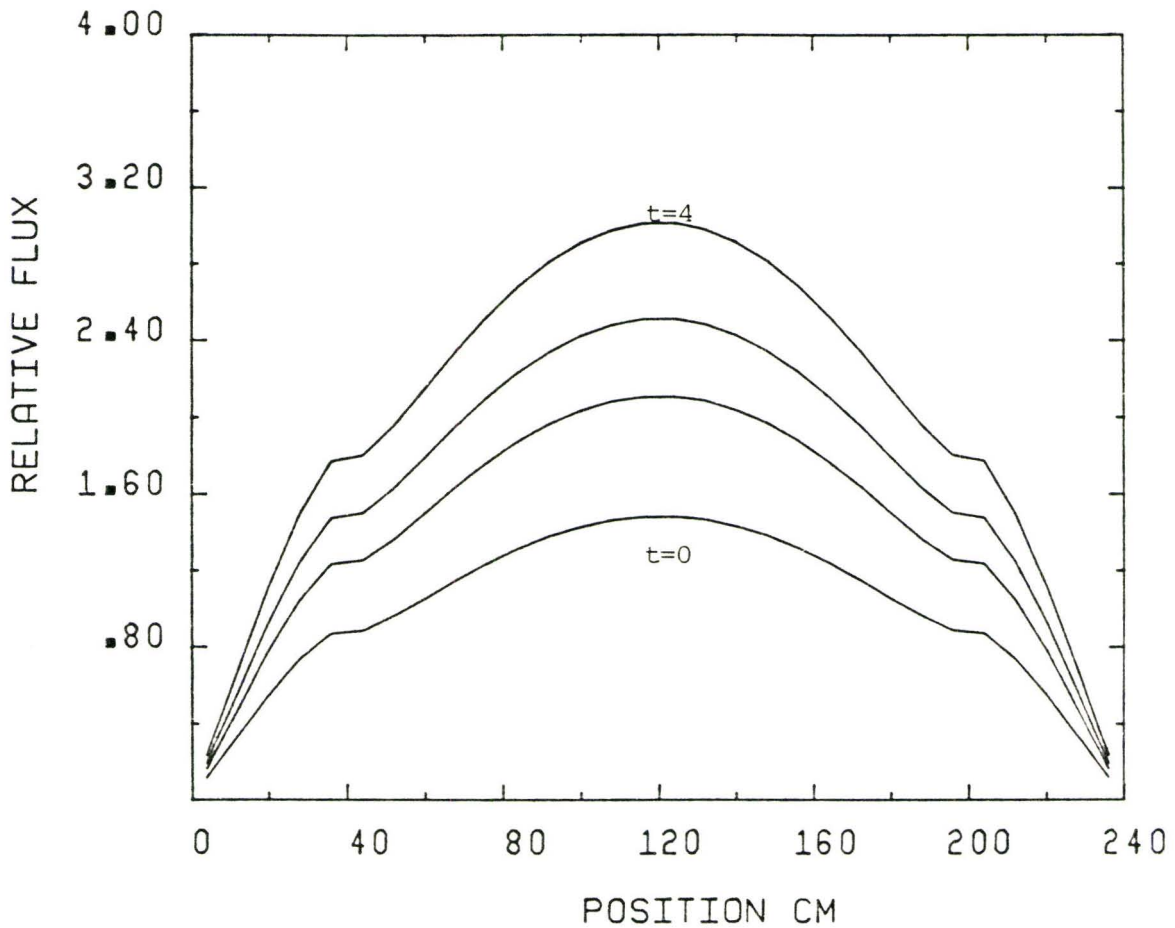
4.00
3.20
2.40
1.60
.80
RELATIVE FLUX
t=4
t=0
0
40
80
120
160
200
240
POSITION CM

Figure 22

Option 3 Results

Convergence and Time Step Criteria: same as option 1

Relative Total Power

Time (sec)	Total Power	Flux Shape Step Iteration Number
0.0	1.000	1
0.1	1.010	12
0.2	1.032	18
0.5	1.134	35
1.0	1.401	62
1.5	1.584	78
2.0	1.682	83
3.0	1.854	91
4.0	2.020	99

Regional Power Fractions: Region 1 and 3 power fractions are zero and region 2 power fractions equal one.

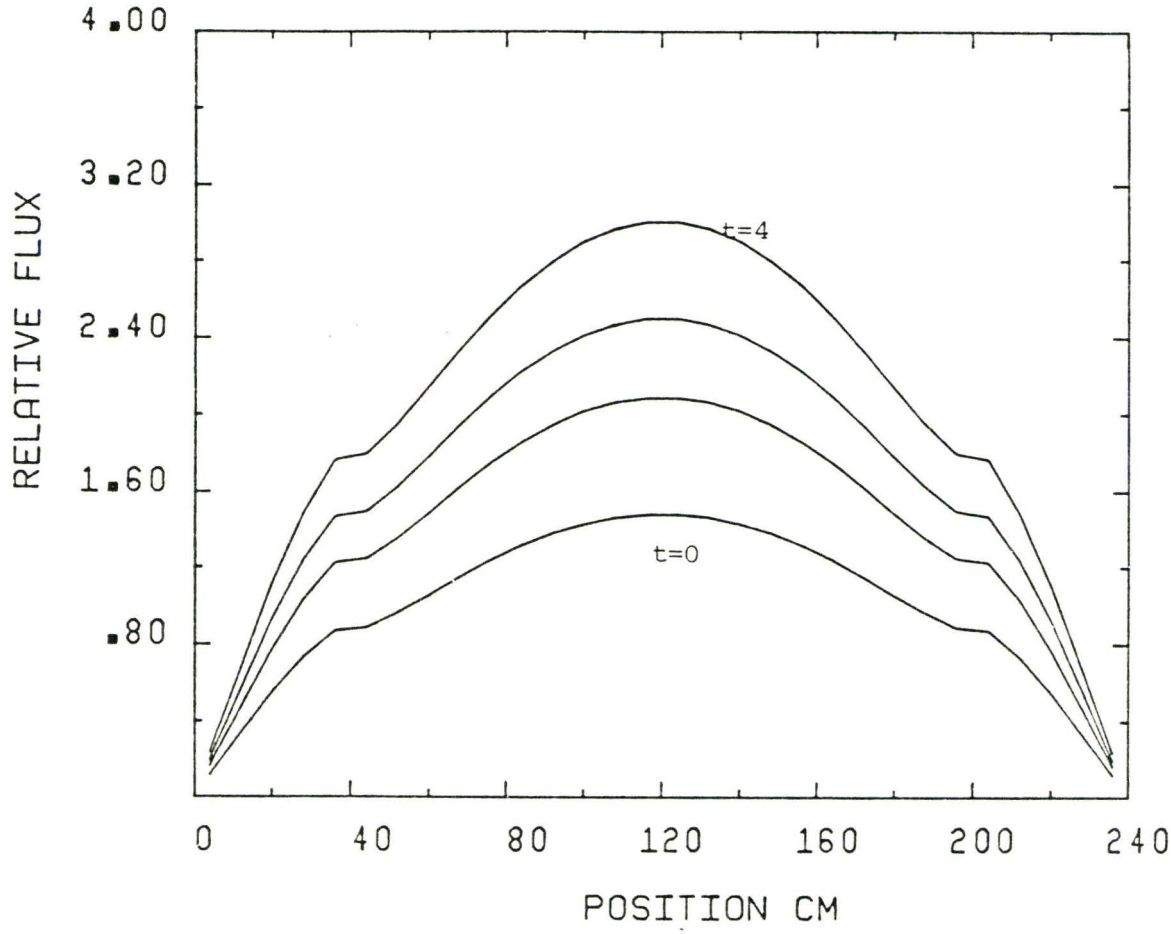
4.00
3.20
2.40
1.60
.80
RELATIVE FLUX
t=4
t=0
0
40
80
120
160
200
240
POSITION CM

Figure 23

Option 4 Results

Convergence and Time Step Criteria: same as option 1

Relative Total Power

Time (sec)	Total Power	Flux Shape Step Iteration Number
0.0	1.000	1
0.1	1.010	12
0.2	1.032	17
0.5	1.137	33
1.0	1.408	63
1.5	1.590	77
2.0	1.687	83
3.0	1.859	91
4.0	2.026	99

Regional Power Fractions: Region 1 and 2 power fractions are zero with region 2 power fractions equal to one.

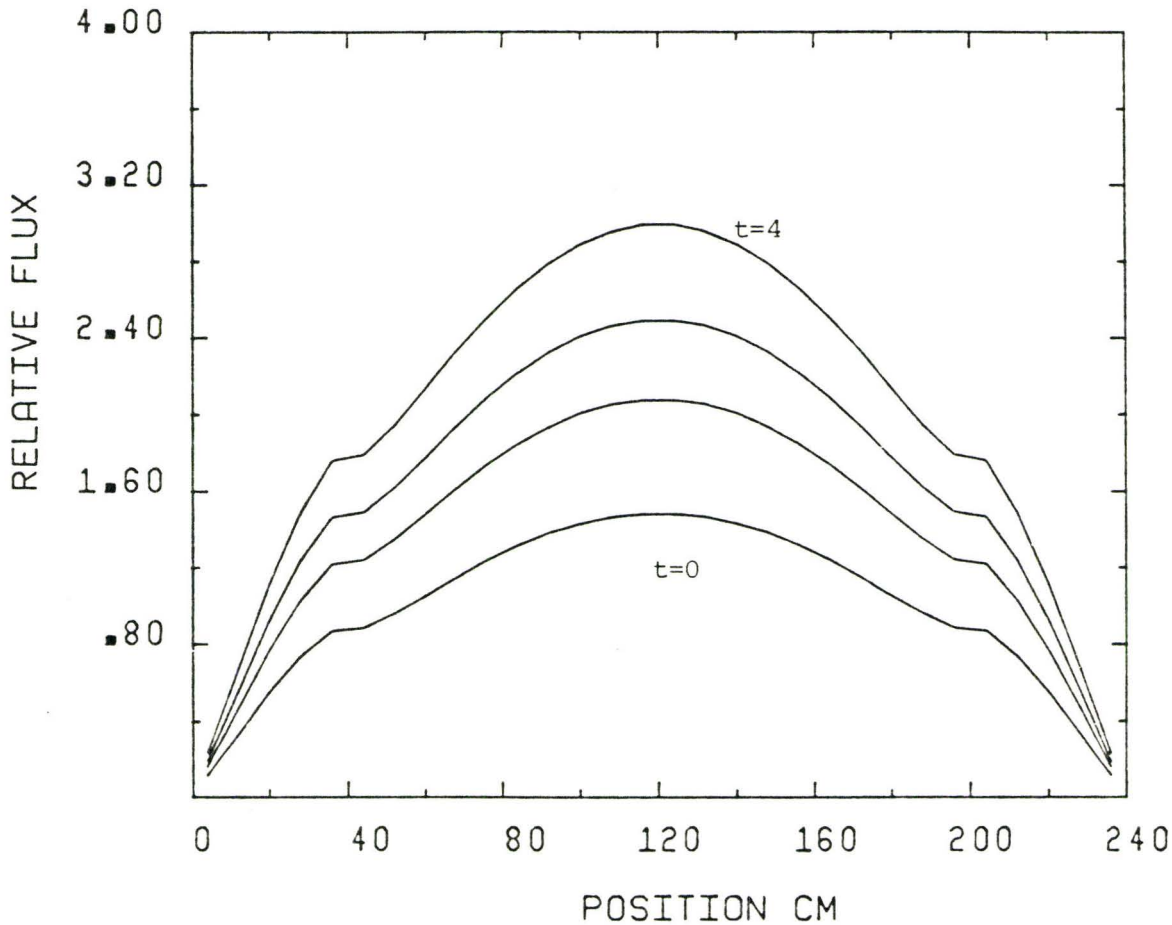
4.00
3.20
2.40
1.60
.80
RELATIVE FLUX
t=4
t=0
0
40
80
120
160
200
240
POSITION CM

Figure 24

References

1. R.S. Varga, Matrix Iterative Analysis, Chapter 3, Prentice Hall, Englewood Cliffs, New Jersey (1962)
2. Weston M. Stacey, Jr., Flux Synthesis Methods in Reactor Physics, Reactor Technology, Volume 15, No. 3, 210-238, (Fall, 1972)
3. K.O. Ott and D.A. Meneley, Accuracy of the Quasistatic Treatment of Spatial Reactor Kinetics, Nuclear Science Eng., 36, 402-411 (1969)
4. J.B. Yasinsky and A.F. Henry, Some Numerical Experiments Concerning Space-Time Reactor Kinetics Behaviour, Nuclear Science Eng., 22, 171-181 (1965)
5. A.F. Henry, Nuclear-Reactor Analysis, Chapter 7, The M.I.T. Press, Cambridge, Massachusetts, and London England (1975)
6. Martin Becker, A Generalized Formulation of Point Nuclear Reactor Kinetics Equations, Nuclear Science Eng., 31, 458-464 (1968)
7. J.J. Kaganove, Numerical Solution of the One Group Space Independent Reactor Kinetics Equations for Neutron Density Given the Excess Reactivity, ANL-6132 (1960)
8. G.K. Leak and A.S. Kennedy, 1D-Diffusion NUC002, ANL-7332 1-93
9. A.F. Henry, Review of Computational Methods for Space Time Kinetics, Proc The Effective Use of Computors in the Nuclear Industry, Knoxville, Tennessee, 3-15, April 21-23 (1969)
10. Benchmark Problem Committee, Argonne Code Center: Benchmark Problem Book, ANL-7416, and Supplements (1977)
11. D.A. Meneley, K.O. Ott and E.S. Wiener, Fast Reactor Kinetics The QX1 Code, Argonne National Laboratory Report ANL-7769 (March 1971)